He Qing

High Voltage Electric Vehicles:

Benefits and Challenges

Master's Thesis

School of Technology and Innovations
Master of Science in Technology
Master's Program in Smart Energy

Vaasa 2024

UNIVERSITY OF VAASA

School of Innovations and Technology

Author: He Qing

Title of the Thesis: High Voltage Electric Vehicles : Benefits and challenges

Degree: Master of Science in Technology

Program: Smart Energy

Supervisor: Mustafa Alrayah Hassan Ibraheem

Year: 2024 **Pages:** 85

ABSTRACT :

Electric vehicles have developed rapidly over the years, because they can reduce carbon emissions and slow down the impact of global warming. On the other hand, their higher energy efficiency and driving experience have also been favored by many consumers. The electric vehicles' (EV) energy efficiency improvement, performance, and the increase of the system voltage are the major interest of many automobile manufacturers, which can maintain or reduce the system current and increase the motor and charging power. In addition, it has a very positive effect on expanding the driving range and charging speed. Compared with the traditional 400V system, the 800V high-voltage system has been widely publicized and studied in recent years, but the specific performance of these two systems under different driving cycles is rare.

This thesis aims to provide a comprehensive dynamic performance comparison between the 400V and 800V EVs system in terms of state of charge (SoC) saving, torque, maxim dc current needed, and charging power. This thesis adopts the mainstream commonly used PMSM motor and FOC control strategy, configures the basic architecture of electric vehicles, and compares its performance in different driving cycles under 400V and 800V systems by increasing the battery voltage, to verify the specific performance of 800V systems.

The thesis findings verified that 800V systems has get better SoC savings comparing to 400V systems, especially during high acceleration speed driving scenarios, whereas the most prominent benefit is the DC current can be decreased significantly with energy efficiency improves. Results also shows the 800V charging system can nearly cut EV battery charging time in half when the current is equal with 400V systems. Challenges for implementing 800V system: infrastructure hinder, SiC semiconductor industrialize maturity, motor and battery technology improvement and future research directions have been concluded and discussed.

KEYWORDS: High voltage, 800V, EV, PMSM, FOC, drive cycle, Battery, Charging, Simulink

ACKNOWLEDGMENTS

I would like to express my grateful gratitude to my supervisor, Dr. Mustafa Alrayah Hassan Ibraheem, for him giving me valuable research directions, key advice and detailed guidance throughout the project, while his course inspired me of this research topic, it was a real honor to complete this thesis under his guidance.

I would also like to express my sincerest thanks to Prof. Hannu Laaksonen, for allowing me to extend my thesis work period when I have medical issues, his support matters a lot throughout my master program.

I would also like to express my deepest gratitude to my family for their support and care during my studies. Special thanks to my wife Quin, my daughter Rosie, and my friends. Thank you for your continued support and encouragement during my studies.

Special thanks to University of Vaasa for giving me the opportunity to participate in this master's degree program, I have gained a lot from many courses in the past two years, which has laid a good foundation for my future academic and career direction.

Contents

Figures

Tables

Abbreviations

BEV	Battery Electric Vehicle
DC	Direct Current
AC	Alternating Current
KWH	Kilowatt-hour
Ah	Ampere-hour
SiC	Silicon Carbide
IGBT	Insulated Gate Bipolar Transistor
MOSFET	Metal Oxide Semiconductor Field Effect Transistor
PMSM	Permanent Magnet Synchronous Motor
IM	Induction Motor
SRM	Switched Reluctance Motor
ICE	Internal combustion Engine
PMW	Pulse Width Modulation
FOC	Field Orientated control
OEM	Original Equipment Manufacturer
PDU	Power Distribution Unit
EMC	Electro Magnetic Compatibility
SoC	State of Charge
SVPWM	Space Vector Pulse Width Modulation
WLTP	Worldwide Harmonized Light Vehicle Test Procedure
EUDC	Extra Urban Driving Cycle
NEDC	New European Driving Cycle
CLTC	China Light-duty Vehicle Test Cycle
CC	Constant Current
CV	Constant Voltage

1 Introduction

1.1 Background and problem

This chapter gives an overview of the thesis topic, discusses the problem, objectives, motivation and research methods chosen for the study and outlining the structure. Also, an introduction to the basics of electric vehicles is reviewed, briefing the background for the thesis's importance.

Climate change and global warming are driving the automotive industry to change to new energy, especially electric vehicles are becoming more and more people's choice. Governments and research institutions in various countries are also encouraging research and development of more efficient and energy-saving solutions to improve the competitiveness and attractiveness of electric vehicles (Liao, Molin, & van Wee, 2016).

At present, there are four types of new energy vehicles (HASAN & ISLAM, 2022): hybrid electric vehicles (HEV), plug-in hybrid electric vehicles (PHEV), fuel cell electric vehicles (FCEV) and pure battery electric vehicles (BEV). This paper focuses on the characteristics of BEV. BEVs do not produce vehicle exhaust emissions and significantly reduce harmful pollutants such as carbon dioxide (CO2) and nitrogen oxides (NOx) compared to conventional vehicles. They reduce dependence on fossil fuels, contribute to enhanced energy security, and promote technological innovation. In addition, the development of BEVs can stimulate economic growth by creating new industries and jobs in areas such as renewable energy, battery manufacturing, and infrastructure.

After about 10 years of rapid development, BEVs have gradually occupied 24% market shares till middle of 2024 in 15 major regions (Marklines, 2024), and the range and charging speed have been greatly improved compared with the earlier versions. At present, most of the BEV architecture is a 400V system, and the corresponding DC fast charging ports are also 400V.

The maximum charging power of the 400V charging is limited to around 100KW (with current 250A). For an electric vehicle equipped with a 100kwh battery, it takes at least 30 minutes to charge from 30% to 80%. The charging speed is still not at a similar level as the refueling speed of traditional cars and which is hindering people's favor on BEVs. Moreover, the battery power and energy efficiency of electric vehicles are desired to be lifted higher and higher to save the energy and extend the mileage.

1.2 Research Motivation

It is said that lifting the voltage architecture of BEV to 800V can improve this situation. According to the formula of power calculation, where P is charging power, V is voltage and A is the current value:

$$P = V \times A \tag{1}$$

Assuming that the charging pile power is 125KW, when the 400V electric vehicle is charged, max current will be 312.5 A, which exceeds the rated value of the 250A cable (Bonnen Battery, 2023), the charging power at this time is limited to 100kW, which cannot fully utilize the 125kW charging station, and when lifting the voltage to 800V, max. current will be 156.25 A, with a cable current rating of less than 250A, the vehicle can fully utilize the 125kW charging power.

In this case, when an electric vehicle with a 100kWh battery, needs 30 minutes to charge 30% to 80% under the current 400V voltage platform and 250A current, it would only need about 15 minutes if the voltage is raised to about 800V, and even faster if extend the current limitation, and this is almost close to the refueling speed of ICE vehicles.

The mileage of the 400V BEV architecture is currently maintained at around 600Km (Electric vehicle database, 2023), and the charging speed is about 100KW, which cannot eliminate the range anxiety of consumers. At the same time, for developers, the energy consumption of the 400V system still has room for compression, for the 100KWH battery,

the weight of the vehicle is about 2 tons (EVbox, Electric car battery weight explained, 2023), while the traditional fuel vehicle is generally about 1.5 tons, the overweight body limits the further improvement of the mileage.

The 800V BEV architecture can improve this situation to a certain extent, for example, it increases the charging speed, which can greatly shorten the waiting time for charging, and at the same time, the energy loss due to heat loss from lower current on drivetrain system is reduced, and the weight of the vehicle is also reduced, which benefit to improve the range of the BEV.

1.3 Literature Review of Studies on High Voltage BEVs

According to research by (Lamm, 2019), high voltage will reduce the vehicle mass especially in battery. Copper is used as a key material for wiring , motors and battery high-voltage busbars in electric vehicles, according to statistics (Copper Development Association INC, 2022), the amount of copper used in a 100KWH BEV is about 80KG, which is equivalent to 4% of the vehicle weight. By increasing the vehicle voltage from 400V to 800V, the current is reduced, the wiring and high-voltage busbar are reduced (Jung, 2017), and the whole vehicle is reduced, the weight of electric vehicles with 800V architecture can be reduced by more than 25KG (Lamm, 2019), as shown in **Figure 1.**

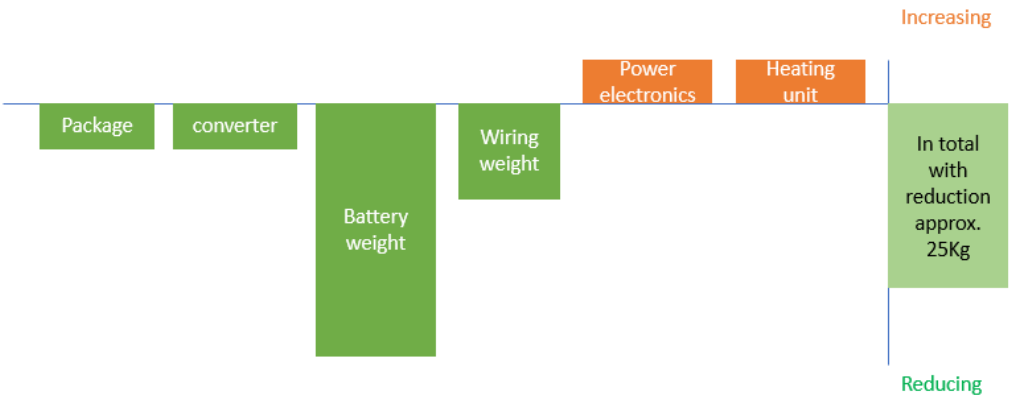

Figure 1. Vehicle mass reduction of 800V topology VS 400V (Lamm, 2019**)**.

With small current, the wires diameters can be reduced, the amount of copper used is then reduced, therefore weight of the whole vehicle is also reduced accordingly.

In research (Jung, 2017), Jung indicated that the DC charging power will be limited between 50KW – 150KW under 400V system, while it can be increased to max. 350KW if charging system voltage increases to 800V. It takes 30mins to charge a 415V battery with 150KW, while it only takes approx. 10mins to charge with 350KW, as shown in **Figure 2**.

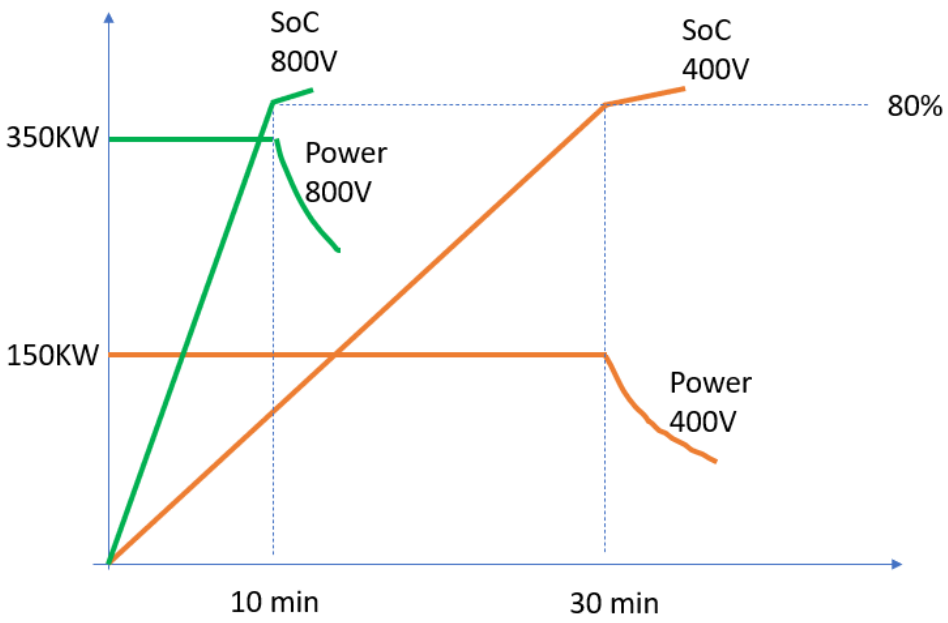

Figure 2. Comparison of charging curve with different charging power **(**Jung**,** 2017**)**.

In addition, the 800V architecture can use SiC MOSFETs instead of Si IGBTs as vehicle power semiconductors, and its losses in the full load range are lower than those of Si IGBTs, and the losses can be reduced by 80% in the normal use range of vehicles, which makes the energy efficiency of SiC high-voltage architecture vehicles about 3.5~8% higher than that of 400V vehicles (Shi, et al., 2023). Study (Allca-Pekarovic, et al., 2024) also shows that BEV's range can increase about 5% under 800V with EPA drive cycles.

1.4 Research Questions and Objectives

The main research questions of this paper are to study the charging rate, energy consumption of BEVs under the 800V high-voltage architecture, and compare with 400V systems to verify their advantages and limitations, to find out the energy consumption characteristics and charging speed of them. Main objectives of this thesis is to research about detail designing of BEV drivetrain system, simulate its performance at the two voltage levels (400V & 800V). Charging systems at two voltage levels will also be investigated and simulated for comparing the charging speed.

1.5 Research Methodology

The research methodology is carried on as listed in **Figure 3**, by simulate the BEV electronic structure in MATLAB Simulink, selecting the PMSM motor with FOC control method, together with lithium-ion Battery, IGBT inverter and the typical 4-wheel vehicle body, run the simulation with different drive cycles, as shown in **Figure 4**. Battery charging is simulated with DC fast charging method in CC (Constant Current) and CV (Constant Voltage) at different phases.

Figure 3. Research process flow chart.

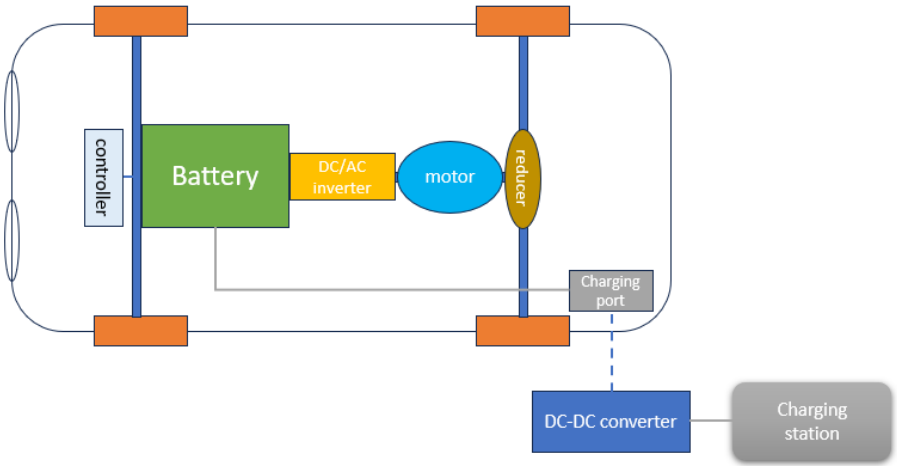

Figure 4. Main components of BEV for the study.

1.6 Research limitations

This thesis focuses on energy efficiency evaluation, and charging speed between 400V and 800V electric vehicle architectures, using the basic structure of BEV and charging electronic circuits, which do not consider complex level of power aspects, such as low voltage (48V, 24V or 12V) accessories, high level motor controlling strategies, regenerative breaking power charging, thermal management and different level braking controlling for passenger comfort, etc. Therefore, the results only indicate the general trend under the technology but may not for very accurate verifications.

1.7 Thesis Outline and Structure

The thesis is organized as follows: Chapter 2 discusses the development of BEV electric architectures and review the details of each sub-system. As well as literature review about the challenges on current technology application and the future developing trend. After that, in Chapter 3, the main sub-systems of BEV and charging circuit are simulated in MATLAB Simulink. In Chapter 4, the results of simulations under different cases are listed and reviewed. Finally, Chapter 5 concludes the thesis, discussing the results and suggesting future research recommendations.

2 Electric Architecture of BEV and Charging Solution

This chapter discusses the main structure of BEV, including Battery, DC-DC converter, DC-AC inverter, Motor, vehicle body as **Figure 5** illustrates, and Charge circuits, including their functions and development trends.

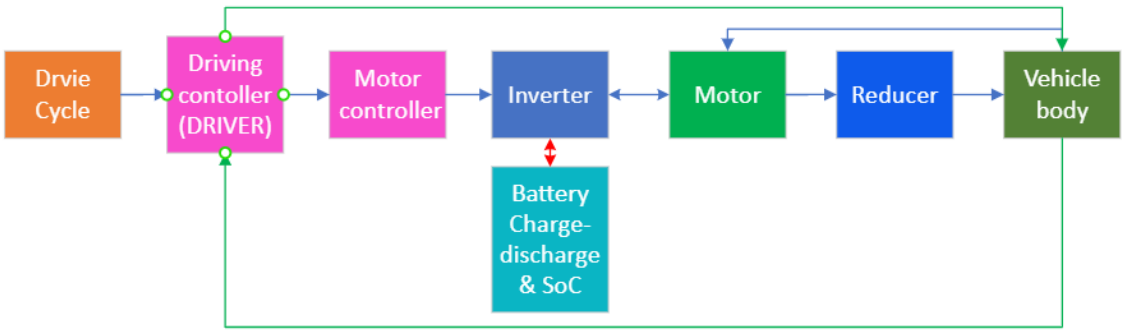

Figure 5. Main structure of a BEV.

The first electric car was developed in the early 1900s (Wikipedia, 2024), although it was far from the electric cars of today. Since then, they have become critical components for a more sustainable society, despite having to surpass engineering challenges. The range, performance (acceleration and high speed), and battery sustainability of these BEVs is still being questioned by consumers today, despite many electric cars having an acceleration speed of 4.x seconds up to 100km/h, while max. speed kept around 200km/h. Meanwhile, with fast upgrading development of batteries, the range of BEVs could now easily reach 500+ km with battery volume over 80 KWH. World car manufacturers are racing into the competition of BEVs while new gamers pop into the market with Highly competitive products, such as Tesla, BYD. To maintain and gain the market shares, they rush into the developing of high efficiency, good power density structures, and fast charging solutions which suit better for consumers' decrement (Aghabali, Kollmeyer, & Bilgin, 800-V Electric Vehicle Powertrains: Review and Analysis of Benefits, Challenges and Future Trends, 2021).

BEVs are powered by electric motors which are fueled by rechargeable batteries. The core structure of a BEV contains several key components: battery pack, electric motor, reducer, power electronics and charging system. Like ICE to traditional vehicles, electric motors are the heart to BEVs.

2.1 Battery

At present, lithium batteries are widely used on high performance BEVs, and it's most common types are, ternary lithium battery and lithium iron phosphate battery, both of which belong to lithium-ion batteries, the difference lies in the difference in cathode materials (Pesaran, 2023).

- Ternary lithium battery refers to the cathode material of lithium nickel cobalt manganese oxide (Li (NiCoMn)O2), which is made of nickel salt, cobalt salt and manganese salt, and the proportion of nickel, cobalt and manganese can be adjusted according to actual needs. The advantage of ternary lithium battery energy is it's dense, and the battery of the same weight can provide a longer cruising range for the vehicle (Yepeng Wang, 2022).
- Lithium iron phosphate batteries are more stable than ternary materials. Its manufacturing cost is lower than ternary lithium batteries, it can be charged quickly and has a long cycle life, and its operating temperature range is also wider. However, the disadvantage is its energy density is much lower than ternary lithium batteries, and its attenuation is worse in low temperature environments (Tredeau & Salameh, 2009). Although lithium iron phosphate batteries have lower energy than ternary lithium batteries under the same weight, they are better in terms of low cost and high safety (Rahul Rao, 2021).

There are also other types of Lithium batteries, such as Lithium cobalt oxide battery (Wu, Zhang, & Lu, 2022), which was used on early version of Tesla Model S BEVs. However, the manufacturing cost of lithium cobalt oxide batteries is high and there is a certain pollution to the environment, which were gradually abandoned. NiMH battery is also a green and environmentally friendly battery with the advantages of high energy density

and long life. It is mainly used in hybrid vehicles such as the Toyota Prius and the Ford Escape. However, nickel-metal hydride batteries are expensive to manufacture and relatively slow to charge (Ying, Gao, Hu, Wu, & Noréus, 2006).

Below **Figure 6** utilizes the characteristics of different batteries materials on the energy density and weight (Tarascon & Armand, 2001).

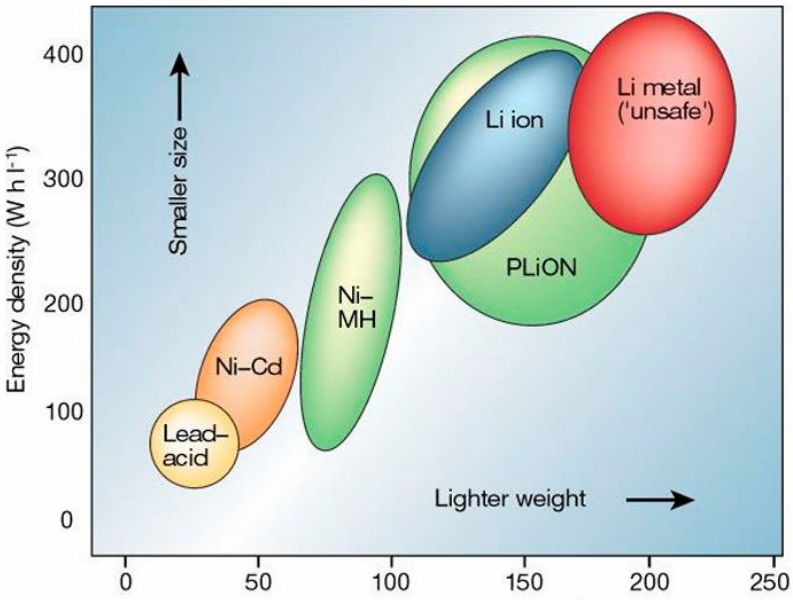

Figure 6. Different types of battery performance (Tarascon & Armand, 2001)

Figure 7 compares the general characteristics and performance of different types of Li-ion batteries as listed below, which illustrate that LFP and NMC are delivering most balanced capabilities on all aspects, while NMC has better energy capacities, LFP has better performance and life-span and safety (Tarascon & Armand, 2001), the type of battery names listed as below:

- Lithium Cobalt Oxide (LiCoO2)
- Lithium Manganese Oxide (LMO)
- Lithium Iron Phosphate (LFP)
- Lithium Nickel Manganese Cobalt Oxide (NMC)
- Lithium Nickel Cobalt Aluminum Oxide (NCA)

- Lithium Titanate (LTO)

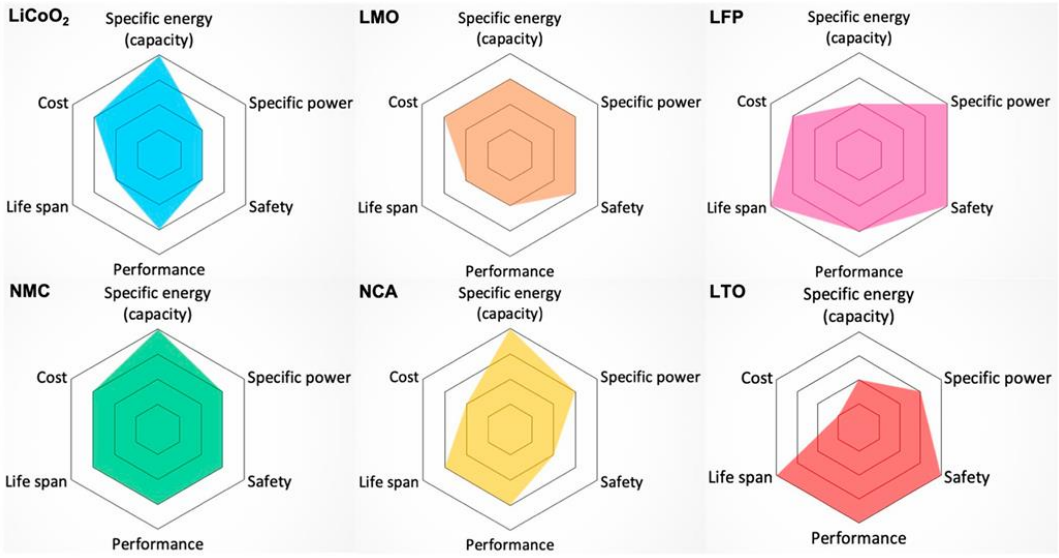

Figure 7. Comparisons of different Li-ion batteries (Tarascon & Armand, 2001).

There are also other types of batteries under research and fast developing, including Solid-state batteries and Graphene batteries. The biggest difference between solid-state batteries and the current mainstream traditional lithium-ion batteries is the electrolyte (Liu, et al., 2024). Solid-state batteries use solid electrolytes to replace the electrolyte and separator of traditional lithium-ion batteries to achieve a higher density battery capacity, and some data show that the volume energy density of solid-state batteries can be increased by more than 70% compared with liquid lithium batteries, reaching 500Wh/kg (Bates, et al., 2022). At the same time, solid-state batteries can also greatly reduce the risk of thermal runaway and have higher safety attributes (Yu, Chen, Gan, Li, & Liquan Chen, 2023). Graphene battery uses two conductive plates coated in a porous material and immersed in an electrolyte solution, which has advantages of ultra-high energy density, long life, and fast charging (Li, Tang, Wang, Zhou, & Linwei Sai, 2024). At present, the specific application of graphene batteries is still in the research and development stage, and no specific models have been announced. However, due to the huge potential of graphene batteries, it has become a research hotspot in the global electric vehicle industry.

2.2 Motor, Powertrain and Transmission

Electric motors offer instant torque delivery, providing smooth and responsive acceleration from a standstill. This characteristic is one of the key advantages of electric propulsion systems, offering impressive performance metrics compared to traditional ICE vehicles. They are generally more compact and lightweight than traditional ICEs, allowing for greater flexibility in vehicle design and packaging. This enables automakers to optimize interior space and improve overall vehicle dynamics. They are also more efficient because of their high transition rate of electrical energy into mechanical power (BAI & Sealy, 2023). Electric motors in BEVs can also function as generators during deceleration, converting kinetic energy back into electrical energy and storing it in the battery. This regenerative braking system helps improve overall efficiency and extends the vehicle's range.

There are many divisions of electric motors used on BEVs. Such as AC motors and DC motors, permanent motors, and induction motors, etc. There are mainly three types of motors are widely used on current BEV's:

(1) Permanent magnetic synchronous motors (PMSMs) are most used because of their excellent efficiency, power density, and torque characteristics. These motors feature permanent magnets embedded in the rotor, providing strong magnetic fields and efficient power conversion.

(2) Induction Motors (IMs) are also a good choice, with the appropriate design and control strategies, while they don't require rare earth materials. IMs offer robust performance and reliability, making them also a good solution for certain high-speed BEV applications.

(3) Switch reluctance motors (SRMs) utilize the magnetic reluctance principle to generate torque and propulsion. Although less common in the automotive industry, SRMs can achieve high speeds and offer benefits such as simple construction, high reliability, and fault tolerance.

According to the research (Aiso & Akatsu, 2022), three types of electric motors for electric vehicle are evaluated while delivering 85KW power, and shows that PMSM act with most high efficiency at both low speed and high speed other than the other two types (SRM and IM) as shown in **Figure 8**.

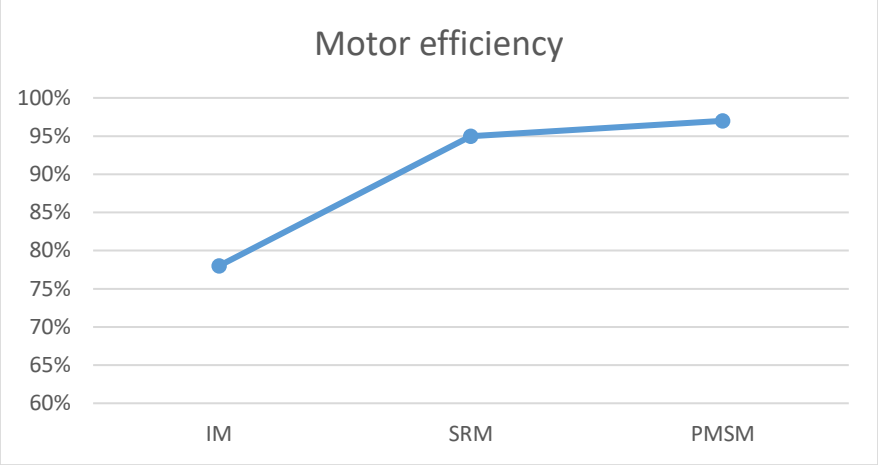

Figure 8. Efficiency comparison for EVs motors. (Aiso & Akatsu, 2022)

A comparison of other characteristics of the three types of electric motors have also been studied and reviewed in the paper (Cao, Mahmoudi, Kahourzade, & W. L. Soong, 2021), and concluded that PMSM has better performance on high speed and torque while IM has advantages on wide range, as shown in **Table 1**.

Table 1. Comparison of three types of electric motors (Cao, Mahmoudi, Kahourzade, & W. L. Soong, 2021).

	PMSM	**SRM**	**IM**
High speed	Good	Good	Good
High torque	Good	Poor	Medium
Torque linearity	Good	Poor	Poor
Power-weight ratio	Good	Medium	Medium
Wide range	Poor	Medium	Good
Low torque ripple	Medium	Poor	Good

The structures of IM, SRM and PMSM are simply illustrated as in **Figure 9**. The stator in an IM features a laminated iron core with three-phase AC windings that create a rotating magnetic field, while its rotor can be either a squirrel-cage type with conductive bars or a wound type connected to slip rings, relying on induced current for rotation. In SRM, the stator has salient poles with concentrated windings that are sequentially energized to create magnetic pull, and the rotor is made of laminated soft magnetic material with salient poles but no windings or magnets, moving to align with the stator poles. The PMSM has a stator like the IM with a laminated iron core and three-phase AC windings, but its rotor contains embedded or surface-mounted permanent magnets, allowing it to rotate synchronously with the stator's magnetic field.

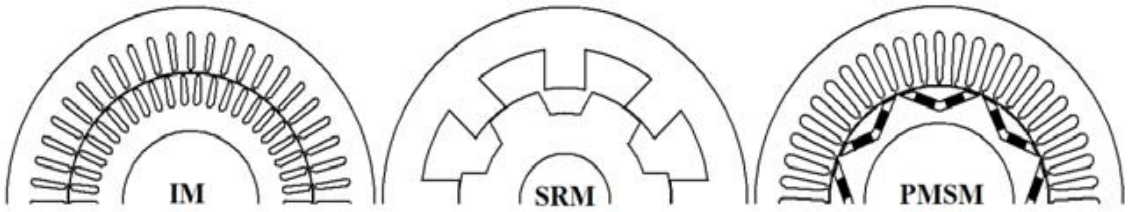

Figure 9 Difference on Motors structures (Cheng, Sun, Buja, & Song, 2015).

Reflection from the market, the PMSM also are widely used as traction motor on electric vehicles as shown in **Table 2** for passenger cars (Krings & Monissen, 2020) , (López, Ibarra, Matallana, Andreu, & Kortabarria, 2019), because of its high efficiency and high-power density. However, due to the rare earth material and high cost, some OEMs such as Tesla are also choosing IM for their high performance BEVs. Others are also developing the SRM solutions, as it is believed that with low manufacturing cost can deliver higher power (Kohei & Kan, 2020).

Table 2. Motor type used on typical BEVs on the current market.

Vehicle	Motor type	Max. speed (rpm)	Power (KW)
BMW i3	PMSM	11400	127
Tesla Model 3	PMSM	18100	202
Jaguar I-Pace	PMSM	13000	147
Chevy bolt	IM	8810	150
Tesla model S	IM	16000	193

This paper selects AC permanent magnet synchronous motor which was widely used on current BEVs as the tractor motor for the EV simulation.

The Transmission model controls the vehicle's shifting requirements throughout gear change, as Motors normally have higher nominal working speed, so transmission is also treated as reducer on BEVs. It shifts torque from the motor model and braking force into front and rear traction forces from driver model. BEV transmissions typically only have one gear reductions between the motor and the wheels for both forward and reverse motion. In comparison with internal combustion engines, which require multiple gear ratios to provide the optimal torque at any given speed, BEVs offer better acceleration for a lighter weight package. Normally the gear ratio is fixed depending on the motor characteristics. The angular velocity of the follower shaft is dividing the ratio with the angular velocity of the input. The follower shaft torque is multiple the input shaft torque.

2.3 DC-AC Inverter

An inverter is a device that converts DC into AC at an adjustable frequency. As the battery is supply electricity in DC, while high power electric motors widely used on BEVs are AC motors, therefore, a DC-AC inverter is needed.

The working principle of the inverter is based on the turn-on and turn-off of semiconductor switches (such as transistors, MOSFETs, IGBTs, etc.), which are switched at a specific frequency and sequence under the precise control of the control circuit, thus realizing the conversion of direct current to alternating current. Inverters can be categorized in many ways, such as voltage type and current type as shown in **Figure 10**.

Voltage-type PWM inverters are mostly used on electric vehicles (Sambhavi & Vijayapriya Ramachandran, 2023).

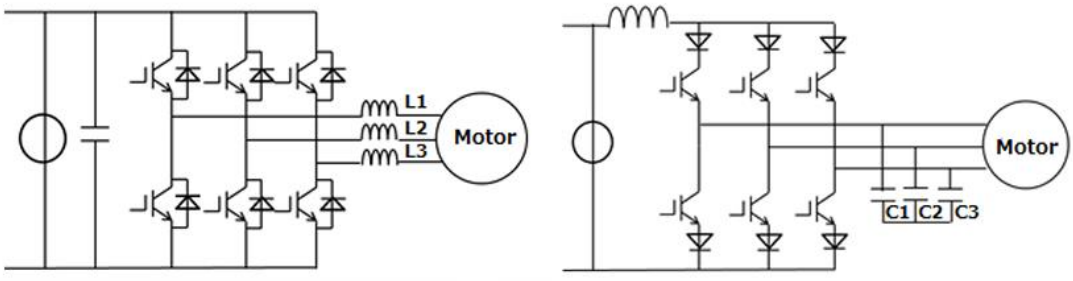

Figure 10. Voltage source inverter and current source inverter.

The main functions of the inverters in the BEVs include three parts: convert the direct current of the battery into three-phase alternating current to drive the motor, change the torque and speed of the motor by changing the voltage and frequency through the inverter, and convert the mechanical energy into electrical energy to charge the battery during regenerative braking, as shown in **Figure 11**.

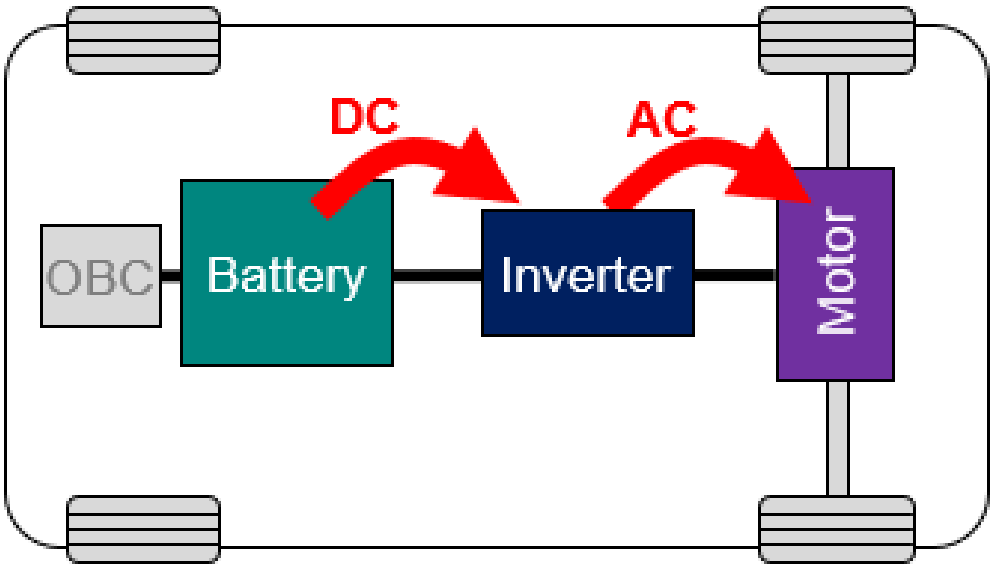

Figure 11. Inverter inside BEV (Panasonic Industry, 2023).

The power module is operated as a switchgear in response to the drive signal while IGBT is normally used due to its high switching capabilities. It can operate at high currents and speeds to meet the high-performance requirements of vehicles. Currently, there is a trend to gradually switch from IGBT to SiC in high-voltage architecture models, which are mainly used in systems above 650V. This is because Si MOSFETs and IGBTs have lower efficiency and performance compared to SiC-based Wide Bandgap devices (Alves, Gomes, Lefranc, Pegado, & Jeannin, 2017). SiC offers higher electric field breakdown capability, better thermal conductivity, higher temperature operation capability, and higher switching frequencies due to the wider electronic bandgap, resulting in lower losses than silicon-based semiconductor devices. SiC materials also minimize switching losses of approx. 66% (TOSHIBA, 2020), as shown in **Figure 12.**

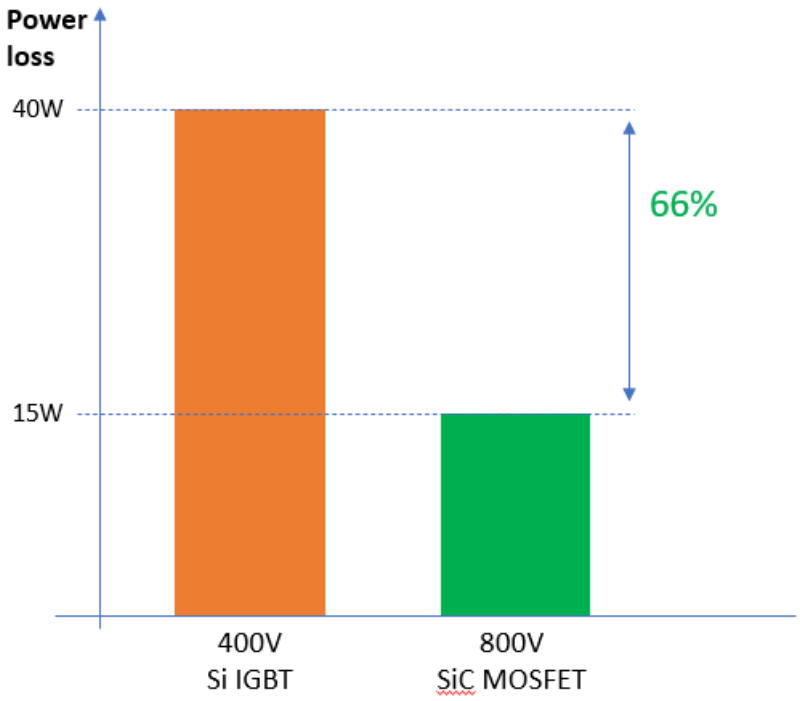

Figure 12. Power loss comparison of Si IGBT and SiC MOSFET (TOSHIBA, 2020).

2.3.1 Controlling of Inverters

The main controlling method used on PMSM controlling are the early constant voltage frequency ratio control, the current commonly used direct torque control, vector control

and other in developing intelligent control. FOC (Field Oriented Control) control technology as typical Vector controlling method, is a PMSM motor control technology widely used in electric vehicles. FOC control technology realizes efficient and high-performance operation of the motor by accurately controlling the stator current and rotor position of the motor. In electric vehicles, FOC control technology can effectively improve the range, efficiency and power density of electric vehicles.

They are mainly used in typical double-ring motor control systems, which generally contain so-called "current loops" and "speed loops". Some of the important modules are mathematical modules such as the "Clark Transform" and "Park Transform", a module for detecting motor current signals, and modules that provide information about the rotational speed and angular position of the motor.

When the electric vehicle performs regenerative braking, the working direction of the inverter is reversed, and it converts the alternating current generated by the electric motor into direct current and feeds it back to the battery. The vehicle slows down when the driver presses the brake pedal or releases the accelerator pedal. At this time, the electric motor no longer consumes electrical energy to propel the vehicle but drives the motor to rotate through the inertia of the wheels, so that it works in power generation mode, converting mechanical energy into alternating current. The frequency and voltage of this alternating current depends on the speed and load of the motor. The rectifier circuit in the inverter converts the alternating current generated by the motor into direct current. This process is the opposite of the inverter process when an electric motor is driven, and a device such as a diode or IGBT (insulated gate bipolar transistor) is usually used to achieve rectification. The rectified direct current is fed back to the battery through the control of the inverter. In this process, the inverter needs to precisely control the magnitude and direction of the current to prevent damage to the battery. In addition, the inverter needs to monitor the status of the battery, such as voltage and temperature, to ensure the safety and efficiency of energy regeneration.

A typical inverter structure consists of the following components: switching device (e.g. IGBT), Bridge circuit, gate driver circuit, control circuit, filter, voltage measurement module, current measurement module, protection circuit and cooling circuit (Barzegarkhoo, Farhangi, Lee, Siwakoti, & Frede Blaabjerg, 2024).

2.4 DC-DC Converter

A DC-DC converter is an electrical device which converts DC sources from one voltage level to another. DC/DC converter, as an important part of the electric power system in BEV, the main function of it is converting the low voltage power such as 12V, 24V or 48V, for power steering systems, air conditioning and other auxiliary equipment. The other role is in the composite power supply system in the charging station, which is connected in series with supercapacitors to regulate the power output and stabilize the bus voltage (Bellur & Kazimierczuk, 2007).

Generally, there are three types of DC-DC converters, non-isolated, isolated, and bidirectional ones. The most popular non-isolated DC-DC converter types are shown in **Figure 13**, the first one is Buck DC-DC converter, which mainly converts high voltage to low voltage (and will increase the current at the same time). In automotive applications, step-down DC-DC converters are used to reduce the high voltage of the main battery (e.g., 400 V) to the lower value (12-14 V) required for vehicle assistance systems (multimedia, navigation, radio, lightning, sensors, etc.). The second one is Boost DC-DC Converter, which can increase the output voltage while decreasing the output current. In some hybrid electric vehicle (HEV) applications, step-up DC-DC converters are used to boost the voltage from the battery, such as from 202 V to 500 V. The third one is Buck-Boost DC-DC converter which can increase or decrease voltage based on the needs of the circuit. The buck-boost converter's output voltage is determined by the input voltage, duty cycle, and switching interval, illustrating how changes in duty cycle directly impact the voltage output (Khan, Nag, Das, & Yoon, 2021).

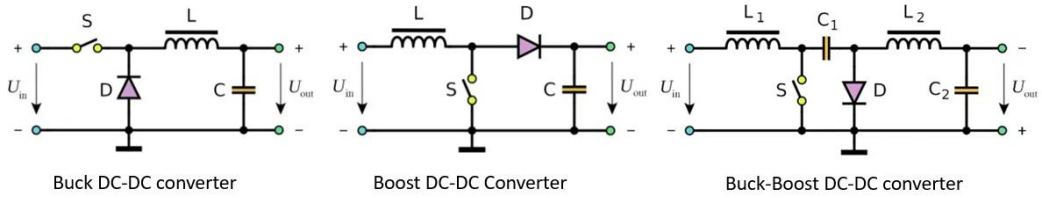

Figure 13. Three types of DC-DC converter (X-engineering, 2015).

The type of converter which is commonly used on electric vehicles are bidirectional DC-DC converters. The topology of a non-isolated bidirectional DC-DC converter is shown in **Figure 14** below. When the battery pack supplies power to the motor, the bidirectional DC-DC converter becomes the Boost converter, which increases the voltage of the battery pack to provide a stable DC voltage to the inverter and reduces the current ripple of the motor. When the motor is in regenerative braking state, the non-isolated bidirectional DC-DC converter becomes a buck converter, which steps down the DC voltage on the inverter side to safely charge the battery pack. In normal operation, only one switch operates at a time between the two power devices of a bidirectional half-bridge converter.

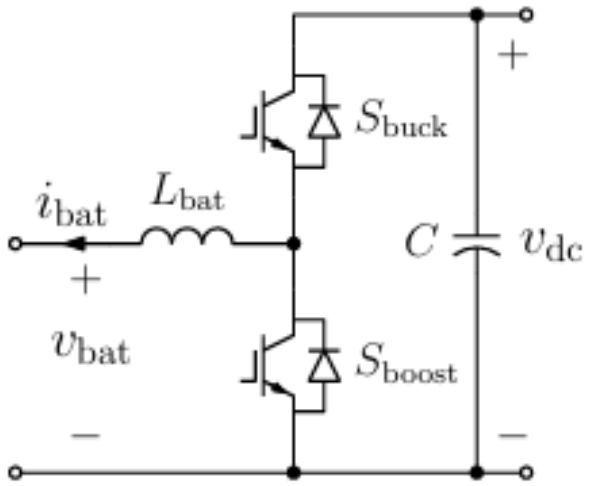

Figure 14. Bi-directional DC-DC converter (X-engineering, 2015).

Adding a high-frequency transformer to a non-isolated bidirectional DC-DC converter can turn it into an isolated bidirectional DC-DC converter, and the circuit topology on both sides of the high-frequency transformer can be full-bridge, half-bridge, push-pull and so on. A typical full-bridge non-isolated DC-DC converter circuit topology (Lüthje, Zhang, Carmen, & Andersen, 2018) is shown as in **Figure 15**. When the energy flows from the high-voltage side to the low-voltage side, the bidirectional DC-DC converter operates in BUCK mode; When energy flows from the low-voltage side to the high-voltage side, the bidirectional dc-dc converter operates in BOOST mode. These isolated bidirectional DC-DC converters use more power switches, which makes them have the advantages of large voltage conversion ratio and galvanic isolation (Singh, Chaudhari, Sekhar, & Kumar, 2023). Therefore, they have advantages over isolated ones for use in electric vehicles, especially in charging solutions.

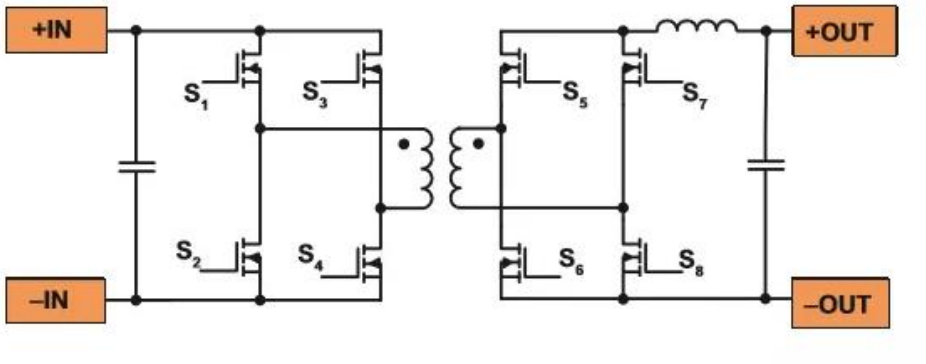

Figure 15. A typical full-bridge non-isolated DC-DC converter circuit topology .

2.5 Battery Charging

The charging system includes DC charging port and AC charging port. The DC charging port is a fast-charging interface, which uses high-voltage direct current, and can be directly delivered to the power battery through the PDU for charging without processing. The AC charging port is a slow charging interface, which uses high-voltage alternating current, which needs to be converted into high-voltage direct current through the On-

Board Charger (OBC) unit and then charged the power battery through the PDU (EVbox, EV charging: the difference between AC and DC, 2023). The connection between the fast and slow charging system and the PDU is shown below in **Figure 16**.

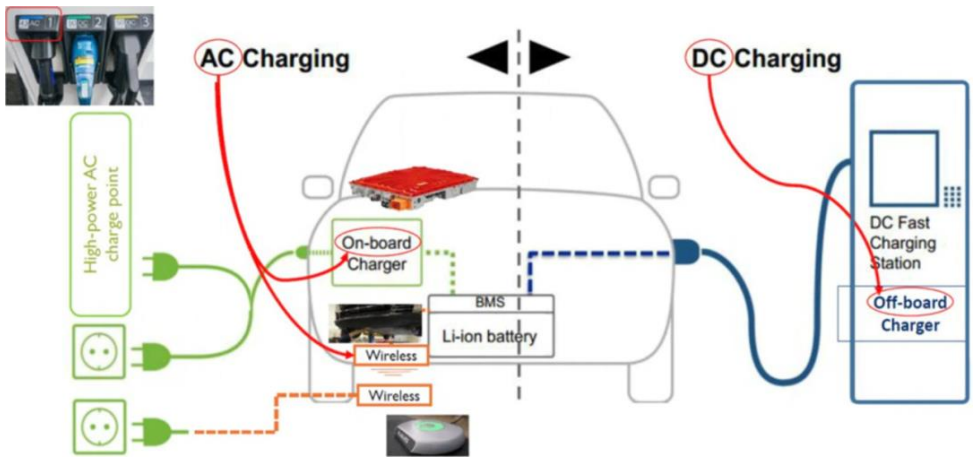

Figure 16. AC and DC charging structure in BEV (Blink, 2022).

The time difference between AC charging and DC fast charging is huge. AC Level 1 charging has a power output of up to 1.4 kW at 12A and 120VAC, while AC Level 2 charging can deliver up to 19.2 kW at 80A and 240V. Theoretically, even with the maximum power level of 19.2 kW AC charging, it would take about five to six hours to fully charge a 100-kWh battery pack. In comparison, with 500A and 400VDC DC fast charging, the same 100kWh battery would theoretically take about 30 minutes to reach full capacity, as shown in **Figure 17**. Charging times will be further reduced as battery technology advances, 800V architecture upgrades, and charging infrastructure improves.

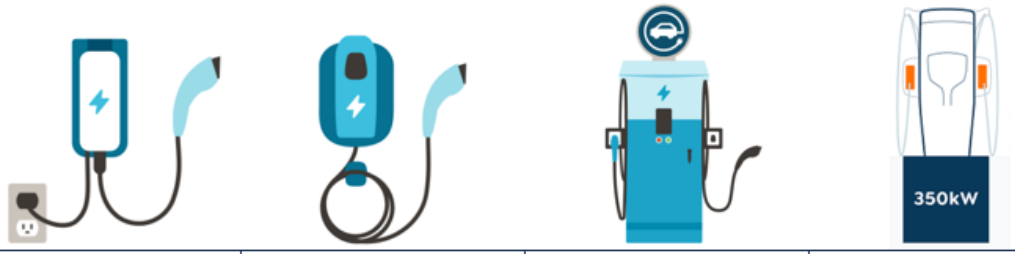

Level 1	Level 2	Level 3	Level 4
Voltage: 120V AC Current: 12-16A Power: 1.4- 1.9KW Charging time: 5-9KM/ hour	Voltage: 240V AC Current: 16-32A Power: 2.5- 7KW Charging time: 16-32KM/ hour	Voltage: 380V DC Current: 125A Power: 40- 150KW Charging time: 20- 30min. to 80%	Voltage: 800V DC Current: 400A Power: 350KW Charging time: 5- 10min. to 80%

Figure 17. Four levels of BEV Charging.

DC fast charging is the charging method especially used at commercial public charging stations. These charging stations convert AC from the grid to DC. When the owner charges an electric vehicle, the DC flows directly to the battery. According to the J1772 standard, the charging current ranges to max. 500A. A typical charging speed curve is illustrated in **Figure 18** below, which the charging speed jumps quickly to top speed in the start periods and keeps in high-speed level until SoC reaches 80%.

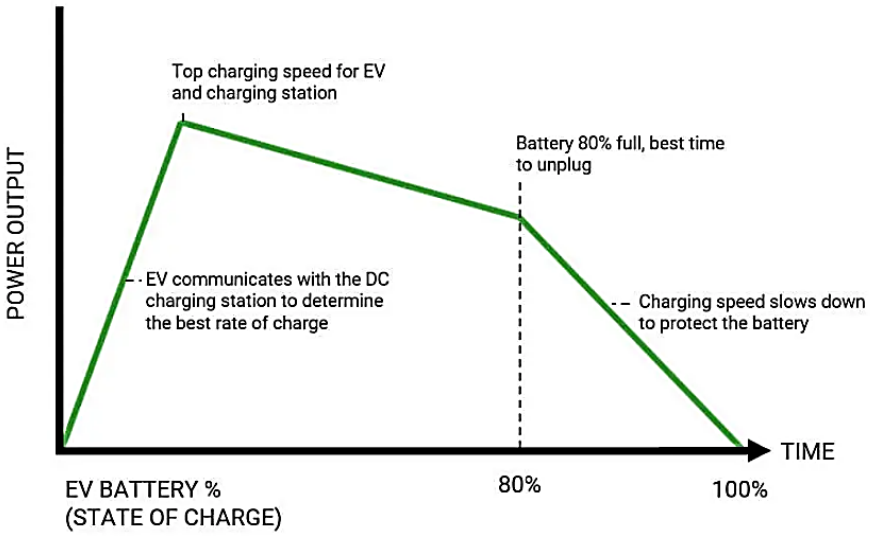

Figure 18. Typical DC fast charging curve (EVEsco, 2023).

As the number of BEV increases, so does the need to create more energy-efficient charging infrastructure systems that can be used to charge vehicles faster, as shown on below **Figure 19**, which the max. charging speed can be realized only when charging station and BEV architectures both meet the Max. charging power capacity.

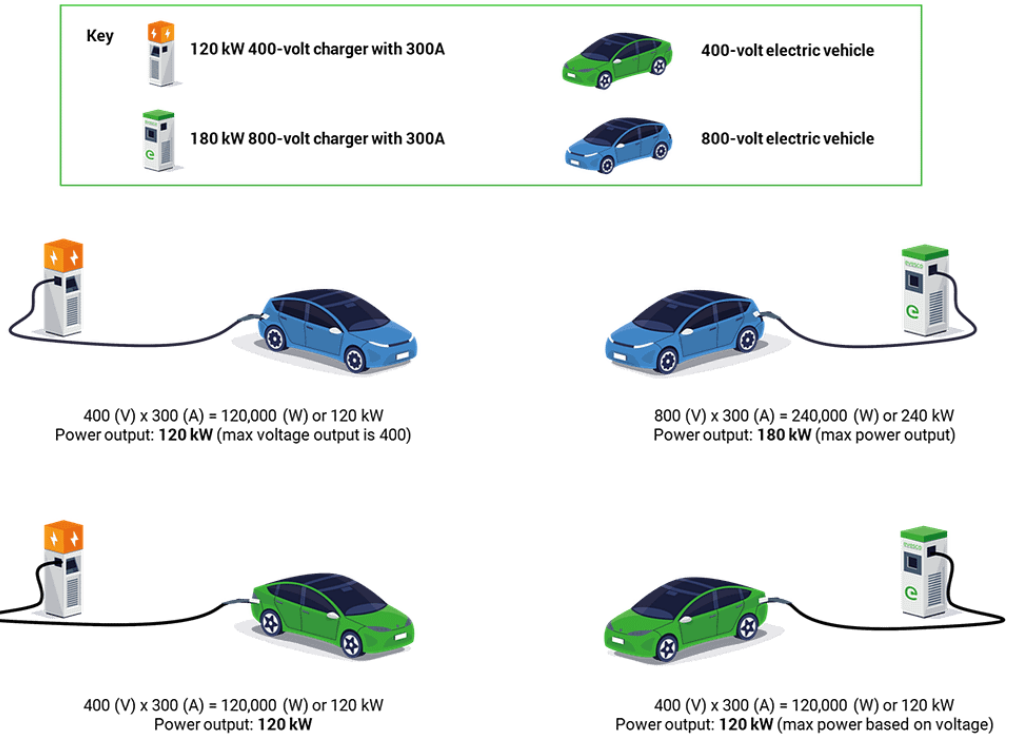

Figure 19. The configuration capable for 800V vehicle charging (EVEsco, 2023).

With a higher driving range and larger battery capacity than previous BEVs, there is a need to develop fast DC charging solutions to meet fast charging requirements. It is calculated that a 150 kW or 200 kW charging station takes about 30 minutes to charge an electric car to 80% for a range of about 250 km (Electrify News, 2023). According to the combined charging system and the most advanced technology, the super-fast DC charging station can provide up to 500 kW of power (Kane, 2023). These super-fast charging stations are working with high voltages to control the current output. High-voltage semiconductor switches (insulated-gate bipolar transistors [IGBTs] and silicon carbide [SiC]) are driving the bus voltage to high levels (800 V or 1,000 V) in the system.

2.6 Developing of High Voltage Batteries and Motors

The sales of electric vehicles are growing globally (IEA, 2024), consumers are expecting better performance on both driving and charging, longer range and faster charging are among their demands (Furcher, Giraldo, Rupalla, & Smith, 2023), and both boil down to the battery. There is numerous research projects focused on solving these challenges, but the most promising one is increasing the battery voltage (Engineering, 2023). Higher battery voltage means more energy and higher charging power, plus increased efficiency, better performance, and weight savings for BEV components such as motors and inverters.

The architecture of a BEV is a sophisticated system comprising batteries, motors, sensors, electronic controls, auxiliary equipment, wiring, and various other components. The battery voltage, whether 400 volts or 800 volts, significantly influences the design and operation of all these elements. Typically, a battery voltage range of 300 to 500 volts is classified as a 400-volt architecture, while a range of 600 to 900 volts corresponds to an 800-volt architecture. Transitioning to an 800-volt architecture involves more than simply connecting batteries to achieve the higher voltage; it also requires redesigning all high-voltage components within the vehicle to accommodate the increased voltage (Engineering, 2023).

The main parameter for charging speed is charger output power, which depends on voltage and current. Increasing the charging current would lead to more heat and energy loss, so increasing the voltage is a better way to increase power and get faster charging. With double the voltage and equal current, a BEV charger could deliver almost twice the energy to BEVs. Of course, the chargers and BEV's converters must be redesigned to be able to carry significantly higher power.

The 800-volt architecture also reduces energy consumption. If a battery outputs the same power as its voltage increases, that means its current must decrease. Since heating and power losses are proportional to the square of the current, heat loss goes down as

voltage goes up. Lower current also has a positive effect on battery aging, thereby extending the battery life.

There are three promising approaches regarding the developing of 800V architectures:

(1) make the entire BEV's high-voltage system operate on 800 volts, eliminating the need for voltage conversion between components. This approach enables faster charging and better efficiency. However, it requires more BEV redesign and higher costs.

(2) have only some essential devices (like the battery pack and drive motor) on 800 volts, with the rest of the system remaining at 400 volts. The need for voltage conversion between 800- and 400-volt devices increases the cost and design complexity and adds conversion power losses. However, this solution requires less BEV redesign and lower costs for the 400 V system, while still enabling faster charging.

(3) a hybrid solution that involves a battery system capable of switching between 800 volts when charging and 400 volts when discharging. Other high-voltage devices remain at 400 volts. This simple and low-cost solution enables faster charging, though discharging at 400 volts means that a reduction in energy consumption will not be achieved.

In addition, most BEVs have no transmission box but use a fixed gear box due to overall weight and cost consideration. Although the electric motor delivers enough power at initial speed phase but will limit the power output at vehicle high speed phase. The maximum speed achievable by a BEV is influenced by the power and torque output of its electric motor. Electric motors deliver instant torque, providing strong acceleration from a standstill. However, as vehicle speed increases, the available torque typically decreases. Thus, the motor's power rating directly impacts the vehicle's top speed potential.

2.6.1 Lighter Weight of Higher Voltage Batteries

A typical structure of a high-voltage battery breaks down as shown below **Figure 20**.

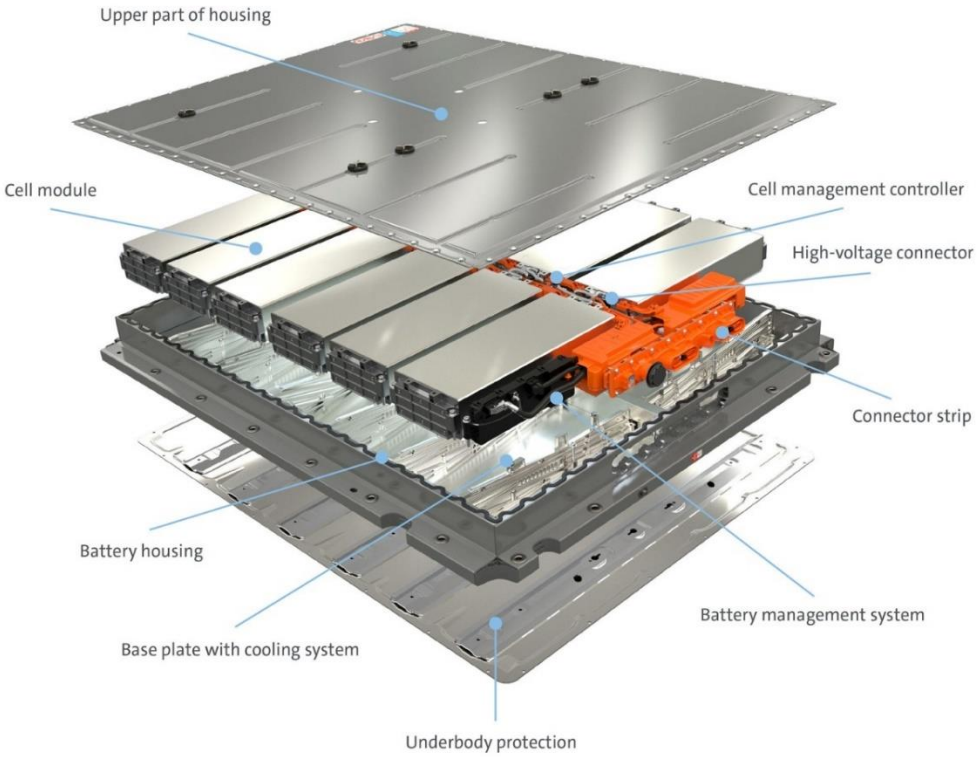

Figure 20. HV battery structure (www.evehicletechnology.com, 2021).

High-voltage battery pack structure mainly include 7 parts:

(1) The battery pack box and cover: it protects all the parts inside, especially the battery, and protects the battery from being crushed.

(2) High voltage wiring harness/busbar: It is to connect the battery module.

(3) Low voltage wiring harness: It is used to collect the cell signal of the battery module, monitor the status of the cell, and then transmit the data to the BMS.

(4) BDU (battery disconnect unit): High voltage power-off system, control the current flow direction, give to different loads, energy distribution unit.

(5) BMS (battery management system): The brain of the battery pack, which consists of the CMU (cell monitoring unit) and the BMU (battery management unit).

(6) Battery module: the most important thing in the entire battery pack, the source of all energy for electric vehicles.
(7) Cooling water plate: part of the thermal management system of the battery pack, which is responsible for the cooling of the battery during heat generation.

The rated voltage of the battery pack is closely related to the multiple high-voltage components of the vehicle, including compressors, drive motors, electronic control modules, PTC, DC-DC, OBC, high-voltage distribution boxes and other components are running under this voltage.

As researched in the report (Lamm, 2019), 800V battery will extremely lighter than 400V ones, because Higher voltage allows for reduced current, which in turn necessitates thinner, lighter wires and conductors. This reduction in current not only lessens the weight of the wiring but also enables a more compact and efficient battery design. Additionally, high-voltage systems are often more efficient in power conversion, which reduces heat and minimizes the need for bulky cooling components. The advanced thermal management systems used in high-voltage batteries are optimized for their specific requirements, contributing to a lighter overall design. Thus, the combination of lower current demands, efficient power conversion, and optimized thermal management results in a lighter and more compact battery system.

2.6.2 High Power of High Voltage Motors

Automotive motors are mainly developed in the following aspects: high power density, diversified development of motor cooling methods, low cost, high integration, good vibration and noise characteristics and high efficiency.

To achieve higher torque density, the motor winding of new energy vehicles has gradually developed from the traditional circular scattered wire winding to the flat copper wire winding. High-speed is the trend of electric vehicle motor development, and

flat wire winding has gradually become the first choice of major electric vehicle manufacturers.

DC motors have been eliminated by the market, switched reluctance motors are still not widely used, and permanent magnet synchronous motors and AC asynchronous motors are widely recognized by the market. As a drive motor, permanent magnet synchronous motor is currently the mainstream choice in the market, and its market share is expected to continue to increase in the future. The speed of the switched reluctance motor can reach more than 15000r/min, and the reliability, torque performance, and power density are also high, but it cannot be widely used at present due to noise, vibration, and other problems.

Permanent Magnet Synchronous Motors are generally preferred over Switched Reluctance Motors and Induction Motors for developing high-power motors for BEVs due to their superior efficiency and performance characteristics. PMSMs utilize permanent magnets embedded in the rotor to create a consistent magnetic field that interacts with the stator’s electromagnetic field, resulting in high torque density and efficient energy conversion. This efficiency translates to better power-to-weight ratios, which is crucial for high-power applications in BEVs. Additionally, PMSMs offer excellent torque characteristics at low speeds and maintain high performance across a broad range of operating conditions, making them ideal for the dynamic demands of electric vehicle driving.

In contrast, Switched Reluctance Motors, while robust and cost-effective, suffer from high torque ripple and acoustic noise, which can affect the smoothness and comfort of the vehicle. SRMs also require complex control systems to manage their operation effectively, adding to the system's complexity and cost. Induction Motors, though durable and reliable, typically exhibit lower efficiency compared to PMSMs due to additional losses in the rotor and the need for more maintenance. They also have lower power density and require external components such as slip rings or brushes for rotor

current management. Thus, PMSMs are generally preferred in high-power BEV applications due to their high efficiency, superior torque characteristics, and reduced maintenance requirements, providing a more refined and powerful driving experience.

From the perspective of product characteristics, permanent magnet synchronous motor and AC asynchronous motor have excellent comprehensive performance, which is the favorite choice for new energy vehicles at present as shown in **Figure 21**.

Figure 21. PMSM motor used on Major Electric Vehicles (MarkLines, n.d.).

3 Challenges on High-Voltage System Implementation

There are some challenges associated with 800V systems, which are mainly related to the endurance of key components such as motors, controllers, and batteries. It requires a change in every connected component, from the battery pack, BMS, connectors, fuses and contactors to drive the inverter power semiconductors, Si IGBTs or SiC MOSFETs (Aghabali, et al., 2020) (Conlon, et al., 2022) (Prasad, Namuduri, & Gopalakrishnan, 2023).

3.1 Protection for Motor Bearing and Electronic Components.

In terms of motors, changing to high voltage, the requirements for bearing corrosion prevention and insulation have increased.

During the high-frequency power switching process, the motor controller will generate induced voltages at both ends of the motor shaft. Under normal circumstances, there is a lubricating oil film between the shaft and the bearing, and this oil film has the effect of insulation. For lower shaft voltages, the lubricant film still has its insulating properties to protect it. When the shaft voltage increases to a certain value and the lubricating oil film in the bearing has not yet been stably formed, the shaft voltage will break through the oil film and discharge. The shaft current is discharged by the shaft through the bearing, and due to the small contact area, high temperature is generated in an instant, which causes the bearing to be partially melted (Zhang, Du, Habetler, & Lu, 2009).

For the 800V system, because its voltage is higher, the voltage change frequency is also higher, the shaft current is larger and the frequency is higher, therefore the bearing anti-corrosion requirements are more important to avoid risk of damage.

At the same time, due to the increase in voltage/switching frequency, the insulation/EMC protection level requirements inside the 800V motor also need to be improved, and for electronic devices, continuous and safe operation at such a high voltage requires better materials and precision processes.

Some possible solutions include using insulated bearings, which are not easily corroded, but the shaft current shaft voltage is still present and may cause damage to other components. Another way is to design a conductive discharge circuit, through the design of a special ultra-high conductivity and wear-resistant conductive fiber ring, one end is connected to the motor housing, and the other end is connected to the motor shaft, forming a low-resistance grounding bypass and discharging current to protect the bearing from electrical corrosion. These design conditions also have strict requirements, such as operating temperature (-50°C~200), maintenance-free, long service life, chemical stability, smoke corrosion resistance, etc.

3.2 Maturity of SiC Semiconductors

800V system has higher requirements for semiconductors, and the current mainstream solution is to use SiC materials, which have excellent performance in withstand voltage, switching frequency, and loss. They are predicted to replace Si-based power semiconductors in future (Sburlan, Vasile, & Tudor, 2021). Taking Si-IGBT as an example, the withstand voltage of Si-IGBT is 650V at 450V, if the electrical architecture of the vehicle is upgraded to 800V, considering factors such as switching voltage switching overload, the corresponding power semiconductor withstand voltage withstand voltage level needs to reach 1200V, and the switching/conduction loss of Si-IGBT increases sharply at high voltage, facing the problem of rising cost and decreasing energy efficiency. However, the detailed performance and environmental resistance of SiC materials need to be further verified. Since SiC is still not comparable to IGBT in terms of capacity and cost, it will take some time for SiC to become fully industrialized.

3.3 High Requirement to Battery Design and Controlling

For 800V rated batteries, in practical applications, due to the consideration of allowing the battery voltage to increase during regenerative braking or normal charging, switching devices with a rated voltage are usually required to be used with more higher

voltage automotive-grade MOSFETs, which are rarely used in the previous 400V platform (Conlon, et al., 2022).

Because the excessive charging voltage or current may cause the stability of the lithium battery electrode material and the electrolyte to be reduced, causing the increase of the internal resistance of the lithium-ion battery, the capacity attenuation and even the potential safety hazards such as fire and explosion. Under the 800V fast charging platform, the charging rate can reach above 4C (Monika, 2023), which puts forward higher requirements for the internal resistance and heat dissipation of the battery cell (the rapid movement of electric ions will naturally produce a lot of heat), and the module level reconsiders the creepage distance, insulation performance, and thermal cooling reliability design (Kucevic, Truong, Jossen, & Hesse, 2018). The voltage levels of the components also need to be increased to more than 800V, while at the same time having to withstand the challenges of high current surges and fast power release. For highly integrated battery distribution units (BDUs), the overall consideration of the liquid cooling solution and the external high-voltage interface is also difficult. Breakthroughs are still needed in battery materials and battery management system (BMS) with high control accuracy.

There are researches to reduce the possibility of lithium precipitation of lithium battery anode due to high pressure, including modifications on oxidation, coating, and etch (Wang, 2022). Such as use non-carbon-based anode materials (Schneider, 2019). Silicon-based materials have a higher potential for lithium intercalation and are less risky for lithium separation, so they can tolerate a higher charging current than carbon batteries.

3.4 Infrastructure Development and Upgradation

Another challenge is the infrastructure, for the 800V charging solutions design, the charging station also needs to achieve the same charging power, which puts forward the need for transformation of the existing charging facilities. Besides, if multiple vehicles use 800V high-power charging power at the same time, its impact on the power grid will be critical, which corresponding energy storage facilities need to be established to reduce the impact.

4 Simulink of BEV and Battery Charging

Electric Vehicles are complex systems in which each component has impacts on overall performance and EMC influence on each other especially of high voltage and current applications. The high-voltage platform technology on electric vehicles can improve the efficiency of the vehicle's drive components and increase the driving range of the vehicle, which can enhance the advantages of electric vehicles in the competition with fuel vehicles. In this chapter, a simulation model of an electric vehicle based on PMSM is built in MATLAB/Simulink, which is mainly composed of four subsystems: a lithium battery with supercapacitor, a permanent magnet synchronous motor, a control system, and a drive cycle with driver. The lithium battery system is used as the energy source while the supercapacitor could contribute to the current stabilizing during battery charging and discharging. As the drive device, the permanent magnet synchronous motor is discussed together with the inverter in the PMSM, and the mathematical model is analyzed more intuitively by establishing a mathematical model, and the coordinate transformation is introduced to simplify the mathematical model, to understand the relationship and law between the parameters of the motor at a deeper level. The electric vehicle acts as a load, and the driver gives acceleration and deceleration commands based on the driving cycle. The following is a detailed analysis of the working principle and simulation model of each device. The structure of the BEV model is created based on some researches (Abulifa, Ahmad, Soh, Radzi, & Hassan, 2017), (Lulhe & Date, 2015), (Carter, et al., 2023) . The results obtained with simulation might not consider all the influencing aspects, but it will give an overview of how the system performs under general conditions.

The overview of the BEV Simulink is built as below **Figure 22**, including drive cycle, driver, controlling unit, inverter, battery, motor, reducer, and vehicle body. With scopes to plot the vehicle speed, battery SoC, torque and battery current and output power.

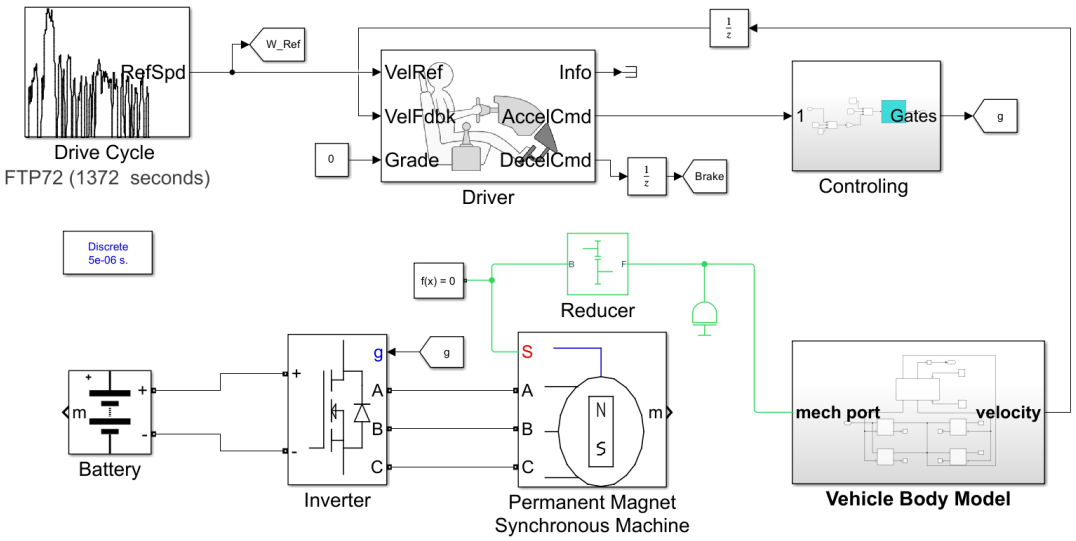

Figure 22. Overview of the BEV model main sub-system.

This chapter firstly develops the simulation in MATLAB Simulink of a typical PMSM equipped electric vehicle, and battery charging circuit. Then run the simulation with 400V and 800V voltages to generate the results.

4.1 Battery

Lithium-ion batteries are used in this model, a standard model from Simulink has been selected, which represents "*a generic dynamic model that represents most popular types of rechargeable batteries*". Equivalent nominal voltages and rated capacities are set so that the battery energy capacities are in same level at the beginning of test. The battery energy capacity can be calculated under below equation:

$$Battery\ Capacity = voltage \times current \times time \tag{2}$$

With high and low voltages and rated capacity to facilitate a 40KWH battery, comparison of the results can be treated in same condition, the SoC of the batteries are set with 80% initially, as shown in below **Table 3**.

Table 3. Battery parameters setting.

Nominal Voltage	nominal capacity	Energy capacity	Initial SoC
400V	100Ah	40KWH	80%
800V	50Ah	40KWH	80%

4.2 PMSM Motor, Inverter and control.

4.2.1 PMSM Motor and Reducer

PSMSM is selected as the drive motor for this simulation for its high efficiency and popularity on the market. The dynamic modeling of a permanent magnet synchronous motor is a high-order differential equation, which is extremely complex to compute, making the following assumptions to obtain its second-order differential equation.

(1) The stator winding current is a three-phase symmetrical sine wave.

(2) Neglecting its high harmonics, core saturation, eddy current and hysteresis losses and temperature effects on motor parameters.

(3) The rotor has no damping windings.

(4) The induced electromotive force in the phase winding is sinusoidal.

The PMSM mathematical model after the Clarke transformation and the Park transformation is as follows. The voltage equation is:

$$U_d = R_s i_d + \frac{d}{dt}\varphi_d - \omega_e \varphi_q \tag{3}$$

$$U_q = R_s i_q + \frac{d}{dt}\varphi_q - \omega_e \varphi_d \tag{4}$$

where U_d , U_q , i_d , i_q, φ_d , φ_q are the d-q axis components of the stator voltage, current, and magnetic chain, respectively. R_s is the stator resistance, ω_e is the rotor angular velocity.

The equations of the magnetic chain are:

$$\varphi_d = L_d i_d + \varphi_f \tag{5}$$

$$\varphi_q = L_q i_q \tag{6}$$

Where L_d, L_q are the inductance of the stator winding d-q axis and φ_f is the rotor permanent magnet chain.

The electromagnetic torque equation is:

$$T_e = \frac{3}{2} P[\varphi_f i_q + (L_d - L_q) i_d i_q] \tag{7}$$

where T_e is the electromagnetic torque of the motor and P is the pole pair number of the motor. In typical conditions, i_d is set as 0, which then the torque is decided by the rotor permanent magnet chain, q axis current and the pole pair numbers.

The mechanical equations of motion are:

$$\frac{J}{P}\frac{d\omega_e}{dt} = T_e - T_L \tag{8}$$

$$T_e = T_L + B\omega_r + JP\omega_r \tag{9}$$

Where T_L is the load torque and J is the moment of inertia, B is the damping coefficient and ω_r is the rotor speed.

In this paper, for the convenience of control analysis, the permanent magnet synchronous motor model in the Simulink library of MATLAB is selected as shown in **Figure 23**. The model is based on the mathematical model in the (d-q) coordinate system. Input the three-phase voltage and load torque from the inverter, and then the stator current, d-q axis current, electromagnetic torque, speed and so on can be output from

the m-port, in this case the mechanical input chooses the rotational port for connection to vehicle body rear tires through reducer.

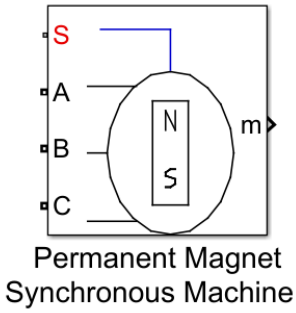

Figure 23. Model of Permanent magnet synchronous motor from Simulink.

The power of the motor is determined by the speed and torque according to formula below, in which P is power of motor, T is the torque, n is the rotation speed:

$$P = \frac{T \times n}{9040} \tag{10}$$

For the same motor, the higher the speed, the lower the torque, and the lower the speed, the higher the torque. When the operating voltage of the motor is increased, the output speed and torque can be maintained by reducing the speed of the motor and increasing the reduction ratio of the reducer to maintain the power of the motor unchanged. In this simulation, the reducer ratio is set with 1.4 in 400V system, and 3 in 800V system to keep efficient drag power for the vehicle.

4.2.2 Controlling of PMSM

The commonly used control methods of permanent magnet synchronous motors are mainly direct torque control and vector control. As the main control strategy of Vetor control, the FOC control method is widely used in the current control, which realizes the control of motor torque (current), speed and position through the control of motor current. FOC has double-loop control (current loop and speed loop) and triple-loop

control (current loop, speed loop and position loop), the inner loop is current loop, the outer loop is speed loop and position loop. Double-loop control can realize the precise control of motor speed by controlling the size of current, the block diagram of the whole dual-loop control is shown in the following **Figure 24**. For an electric vehicle that operates, the speed is controlled by the driver, so there is no speed loop, only a current loop. The driver decides to accelerate and decelerate according to the current speed and the required speed, and sends the corresponding torque command value to the motor control system, and the motor drive system calculates the required Id and iq current according to this torque command, and then controls the motor acceleration and deceleration (Hailin, Shirong, hongtao, Zhan, & Fuyuan, 2019). In the case of electric vehicles, which require high real-time performance, the current is often calculated by the command current lookup method. In this case, to simplify the controlling, driver acceleration signal been transferred into direct iq_ref to control the motor current for speed increase and decrease.

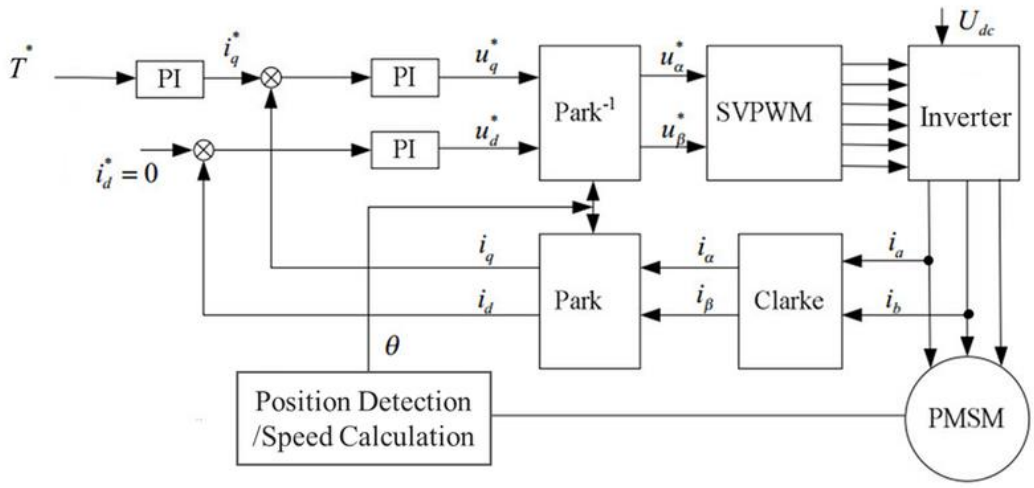

Figure 24. FOC Control diagram of PMSM.

The inner loop of the FOC in is divided into several steps including three coordinate systems (three-phase stationary coordinate system (A-B-C), two-phase stationary coordinate system (α-β), and rotating coordinate system (d-q)), three methods of coordinate transformations (Clark transformations, Park transformations, and inverse

Park transformations), one control algorithm (PID control algorithm) and a method of pulse-width modulation (SVPWM).

The process of FOC control is stated as below:

(1) Collect three-phase currents I_A, I_B, I_C;

(2) Clark transforms the three-phase currents to get the currents I_α, I_β under the two-phase stationary coordinate system.

$$I_\alpha = I_a - I_b cos\frac{\pi}{3} - I_c cos\frac{\pi}{3} \quad (11)$$

$$I_\beta = I_b cos\frac{\pi}{6} - I_c \cos\frac{\pi}{6} \quad (12)$$

(3) And then I_α, I_β for Park transformation to get the rotating coordinate system under the current, i_d , i_q;

$$i_d = I_\alpha \cos(\theta) + I_\beta \sin(\theta) \quad (13)$$

$$i_q = -I_\alpha \sin(\theta) + I_\beta \cos(\theta) \quad (14)$$

(4) Get the rotor speed and angle θ;

(5) Calculate the error between the actual rotational speed of the rotor, and the set target speed.

(6) Throw the error into the PI controller, the actuator output i_{q_ref};

(7) Calculate i_d , i_q and the set value of i_{d_ref}, i_{q_ref} error.

(8) Throw the error into the PI controller and the actuator outputs U_d and U_q respectively.

$$V_d = V_\alpha \cos(\theta) + V_\beta \sin(\theta) \quad (15)$$

$$V_q = -V_\alpha \sin(\theta) + V_\beta \cos(\theta) \quad (16)$$

(9) U_d, U_q undergoes inverse Park transformation to obtain U_α, U_β ;

$$V_\alpha = V_d \cos(\theta) - V_q \sin(\theta) \quad (17)$$

$$V_\beta = V_d \sin(\theta) + V_q \cos(\theta) \quad (18)$$

(10) Finally, U_α, U_β go through SVPWM to calculate the voltage vector action time applied by the selected voltage vector to output the signal for inverter switching control.

The detail FOC control model is set as below **Figure 25** as typical FOC control diagram:

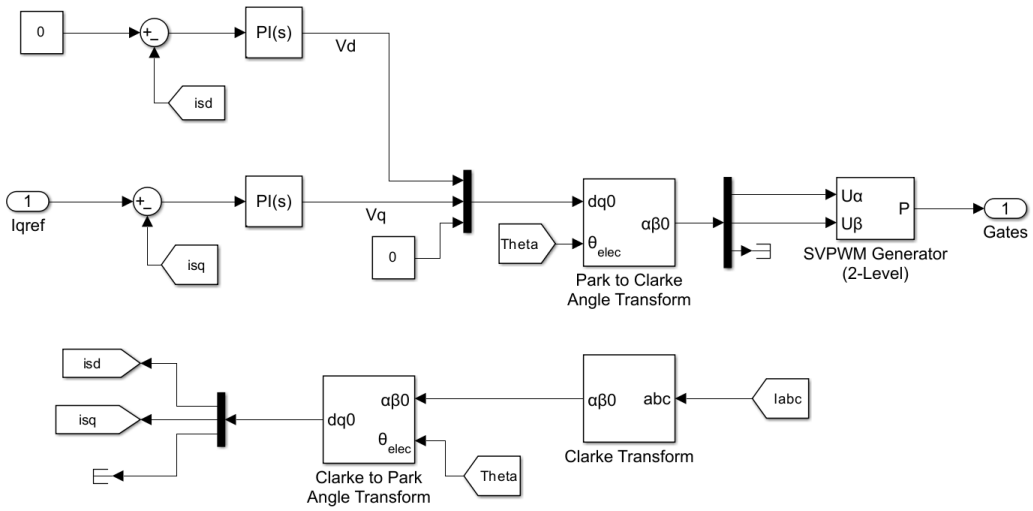

Figure 25. FOC control algorithm in Simulink.

As the drive cycle is applied in this model, so the regenerative braking control logic has been considered, which include the switch to control the drive or brake mode of the vehicle and use PWM generator simulate pulses for the inverter control during regenerative braking. The detail regenerative braking control logic is set as below **Figure 26,** during braking, iq_ref switch to negative value for motor current direction reverse and charging energy back to battery. The pulses are generated through FOC control algorithm during acceleration, while pulses are generated through the braking signals via PWM generator.

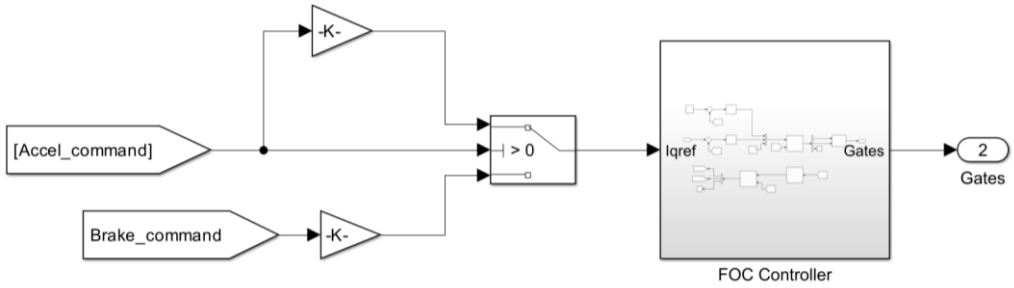

Figure 26. regenerative braking control logic in Simulink.

4.2.3 Inverter

The pulse signal generated after the FOC controlling, then to control the switching state of the inverter, this step replaces the switching table in the traditional direct torque. Then the inverter outputs three-phase voltage and current for the normal operation of the permanent magnet synchronous motor, currently, the three-phase current is collected, which is used for the calculation of the torque and the magnetic chain and is fed back to the given, to complete the whole permanent magnet synchronous motor double closed-loop control system. The inverter uses the standard universal bridge module in the Simulink, which converts DC into AC during motor driving mode, and converts DC into AC during motor generator mode. Typical IGBT/Diodes mode is selected, as mostly used on the market, as **Figure 27** shows.

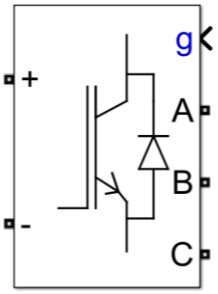

Figure 27. Inverter module from Simulink.

4.3 Vehicle body

To calculate the total power requirements is to determine the forces acting on the vehicles, in this study a BEV of standard rear single motor is used as an assumption.

The total force on the vehicle is the sum of all the forces given above and as follows：

$$F_{total} = F_{rollling} + F_{aerodynamic} + F_{gradient} + F_{acceleration} \quad (19)$$

While:

$$F_{rolling} = m \times g \times f \quad (20)$$

which m is the mass of vehicle, g is the f is the rolling resistance coefficient.

$$F_{aerodynamic} = \frac{C_D \times A \times V^2}{21.15} \quad (21)$$

which V is the vehicle velocity, CD is the coefficient of air resistance, A is the front area of the vehicle.

$$F_{gradient} = m \times g \times sin\alpha \quad (22)$$

which α is the slope angle.

$$F_{acceleration} = m \times a \tag{23}$$

which a is the acceleration speed of the vehicle.

Modules from Simulink of vehicle body, wheels, are selected for configurating the vehicle model (Nayak, Bohre, & Kumar, 2022), as shown below **Figure 28**.

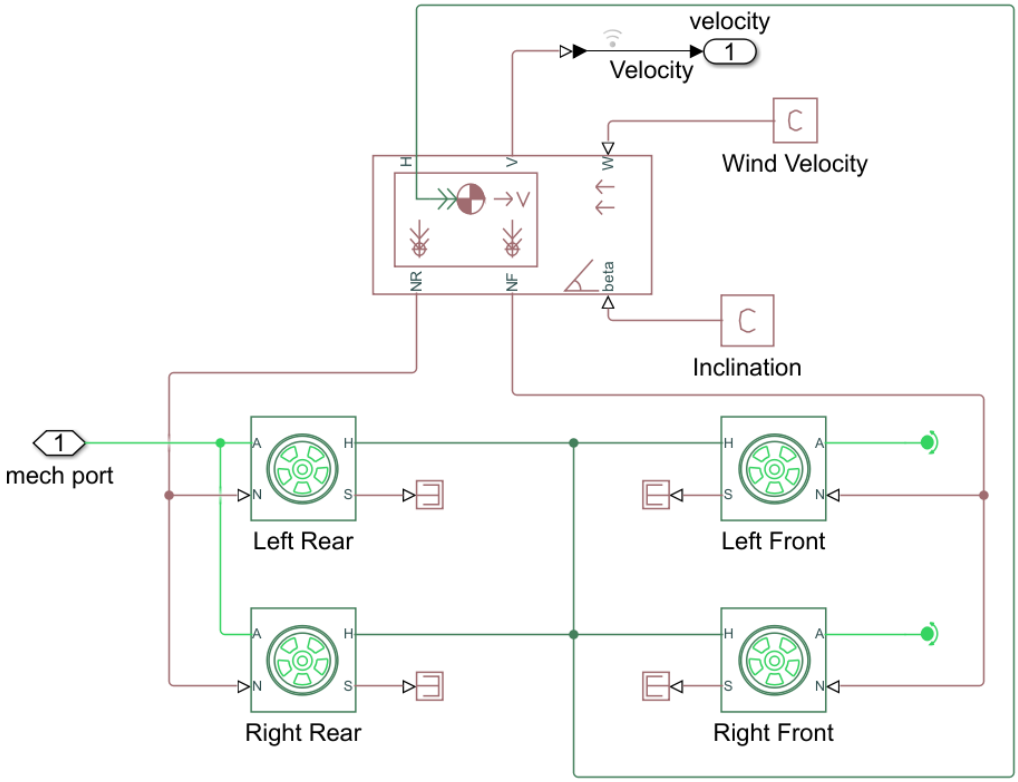

Figure 28. Simulation of vehicle body in Simulink.

The models configurated for this study do not represent any environmental dynamic influence. For this reason, the configuration of each element is chosen as standard ones. The vehicle data sheet chosen based on a typical BEV with rear driving single motor, which datasheet stated as below **Table 4**. 1800kg is the average weight of the BEV Passenger car on the market with a front area of 2.4 m2. The Passenger vehicles have a

drag coefficient of between 0.3~ 0.6, in this case 0.4 is chosen as an average value. For the Motor in this simulation, Gear ratio of 3 is selected for better performance.

Table 4. BEV vehicle body parameter.

Parameter	Value
Mass of vehicle	1800 kg
Wheel radius	0.35 m
Vehicle front area	2.4 m^2
Rolling resistance coefficient	0.015
Drag coefficient	0.4

4.4 Drive Cycle and Driver

Drive cycles are speed-time graphs used to calculate vehicle exhaust emissions and fuel consumptions. It can be used in this study to simulate the performance of vehicles under different driving circumstances. EUDC, WLTP, FTP75 and other specific drive cycles have been applied for evaluate BEV's range performance as it contains strict driving situations stimulate different road driving, example of NEDC (New Eupean Driving Cycle) plot as in **Figure 29**.

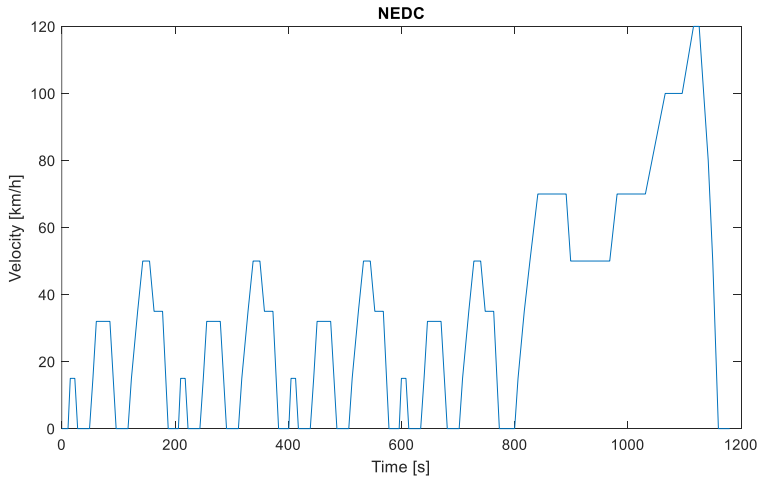

Figure 29. Drive cycle of NEDC.

The features of typical drive cycles are listed in below **Table 5**, which include duration, average speed, total distance (Banuri, Qayyum, Qureshi, & Ahmed, 2020):

Table 5. Features of different driving cycles.

Features	Japanese 10	EUDC	NEDC	WLTP class 1	FTP75	China CLTC	India Drive cycle	High speed (specific)
Time (s)	135	400	1180	1022	1874	1800	108	85
Average speed (km/h)	17.7	62.59	33.35	27.6	17.77	28.96	21.93	60
Max. speed (Km/h)	40	120	120	64.4	91.25	114	42	120
Max. Acceleration speed (m/s^2)	0.79	0.83	1.06	0.76	1.48	1.47	0.61	0.83
Total distance (km)	0.664	6.95	10.93	8.09	17.77	14.48	3.948	1.434

The Longitudinal Driver block (**Figure 30**) inside Simulink implements a longitudinal speed-tracking controller. Based on reference and feedback velocities, the block generates normalized acceleration and braking commands that can vary from 0 through 1. It can be used to model the dynamic response of a driver or to generate the commands necessary to track a longitudinal drive cycle. The "*Predictive* control" type is selected for driver steering control behavior during path-following and obstacle avoidance maneuvers. Drivers preview (look ahead) to follow a predefined path.

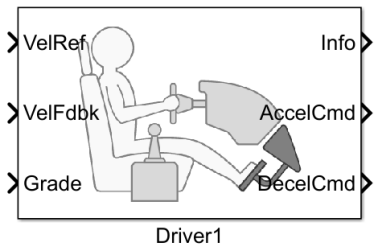

Figure 30. Driver model from Simulink.

4.5 Simulation of Battery Charging Circuit

The main way applied to BEV lithium battery fast charging is the combination of CC (constant current) and CV (constant voltage) charging modes, as shown in **Figure 31.** In the initial stage, in order to quickly increase the charging rate, a large constant current is set for charging, and the voltage of the battery rises slowly in this process, this stage is the constant current phase, when the battery voltage or SoC rises to the set value, it will switch to constant voltage mode, at this time, the voltage remains constant, the current gradually decreases, and the charging power is gradually reduced. Until it reaches a near-full state, it is then floated up with a small amount of power to protect the battery.

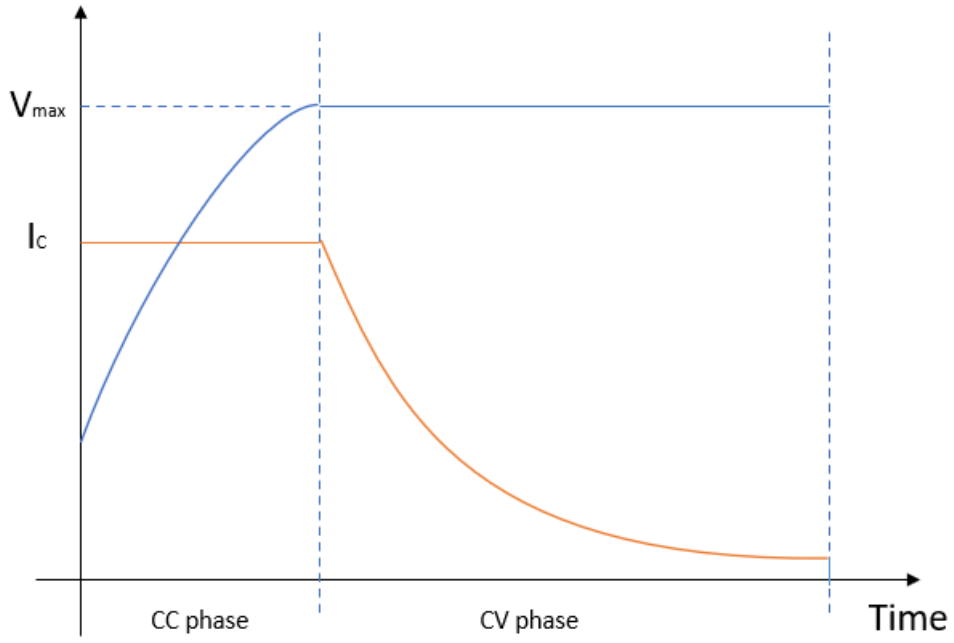

Figure 31. CC and CV charging mode for battery.

The controlling flow is shown below in **Figure 32**, during the charging start, some battery protection measurements are done to maintain the battery in good condition, such as temperature, voltage, etc. And then compare the voltage with set value to decide the charging mode, monitoring the status during the charging period, and finally stop

charging when battery voltage, SoC or temperature reach set value (Shen, Vo, & Kapoor, 2012).

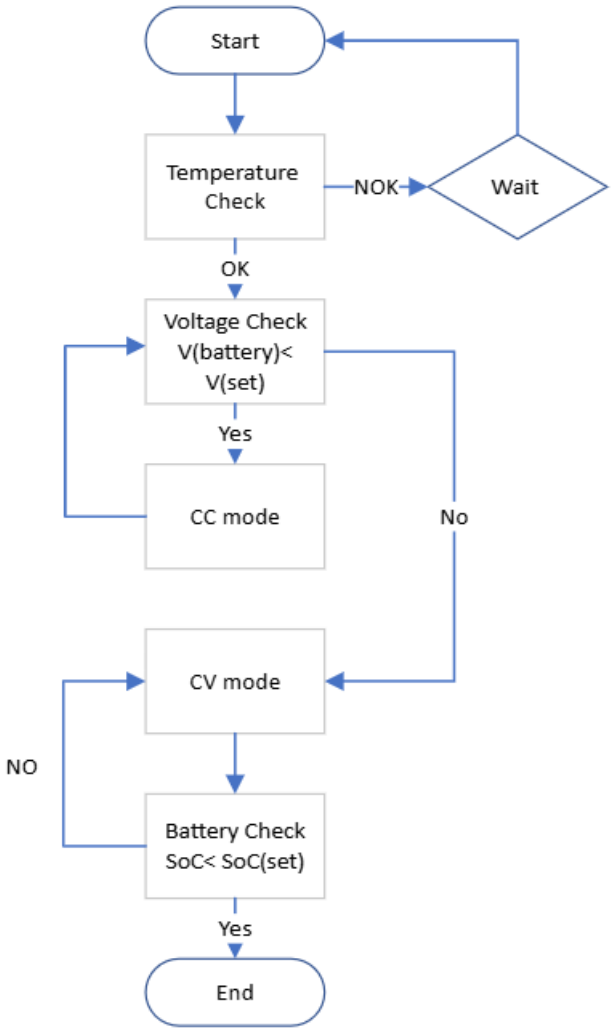

Figure 32. Battery DC fast charging controlling flow.

Detail simulation is generated as in **Figure 33**. A model of battery charging has been simulated to evaluate the charging speed of high voltage and low voltage DC charging station. The model includes modules of DC voltage source, IGBT generate the voltage levels for battery charging, PWM pulse generating, and control system controlling the voltage and current of charging, based on the reference introduced in paper (Arancibia & Strunz, 2012) and (Yuexian, Tianyu, Yayu, & Xiaoru, 2014). The model built in Simulink

is shown below **Figure 34**. By setting high charging voltage to evaluate the battery charging speed compared to lower voltage levels.

The charging power parameters are set below **Table 6**. For 400V Li-ion battery, fully charged voltage is 465V, therefore the Max. charging voltage source is set as 466V. For 800V Li-ion battery, fully charged voltage is 931V, therefore the Max. charging voltage source is set as 940V and 1000V. Difference Current values are set for 800V charging system between 150A to 350A for evaluating the charging power influences. Battery volume varies between 400V and 800V, both of their capacities are set with 40Kwh.

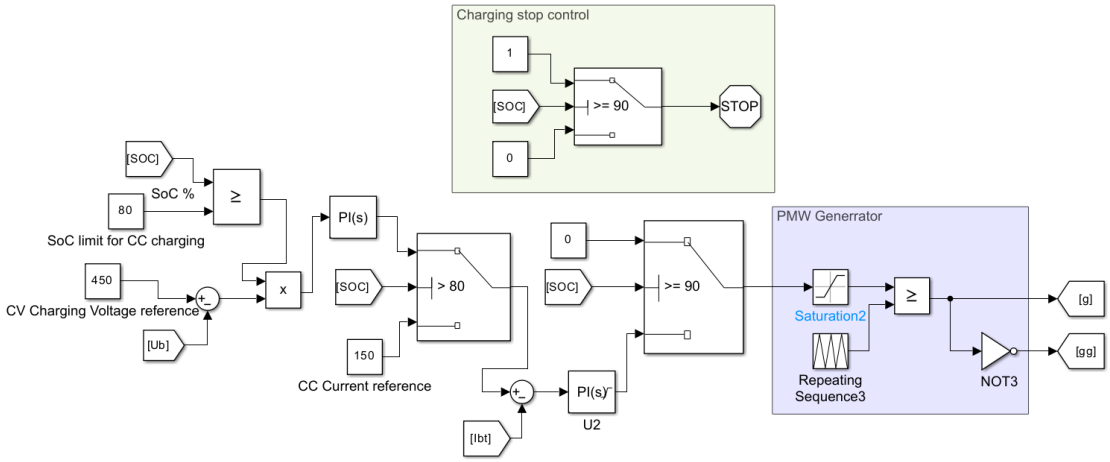

Figure 33. Charging controlling algorithm.

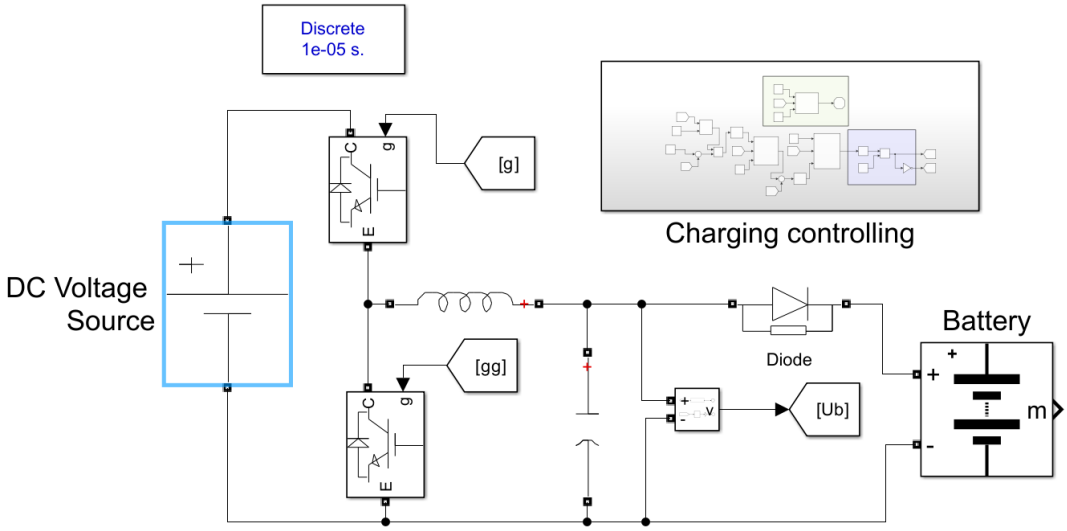

Figure 34. BEV battery DC charging Simulink.

Table 6. Charging parameters for 400V and 800V battery

Battery voltage	**400V**	**800V**	**800V**	**800V**
Charging power(max.)	139.8KW	141KW	300KW	350KW
Charging voltage (max.)	466V	940V	1000V	1000V
Current (max.)	300A	150A	300A	350A
SoC initial	20%	20%	20%	20%
SoC end	90%	90%	90%	90%
Battery volume	100Ah	50Ah	50Ah	50Ah
Battery capacity	40Kwh	40Kwh	40Kwh	40Kwh

5 Simulation Results and Discussion

This chapter reveals the simulation results built in chapter 4 as introduced. The data of SoC of battery, vehicle speed, torque of motor and DC current are collected to compare the performance of the systems. The initial state of charge of the battery are same from 80%, the final state of charge after each driving cycles are collected in **Table 7**.

Table 7. SoC changes after different drive cycles (initial state of charge 80%).

	India	JAPAN	High speed cycle	WLTP	EUDC	NEDC	CLTC-P	FTP75
400V SoC(%)	79.42	79.15	77.48	76.92	76.23	71.72	68.04	57.97
800V SoC(%)	79.68	79.58	78.49	77.58	77.07	74.69	73.03	69.52
SoC saving (800V VS 400V)	0.26	0.43	1.01	0.66	0.84	2.97	4.99	11.55

The SoC savings on 800V system compare to 400V system are listed and illustrated in **Figure 35**.

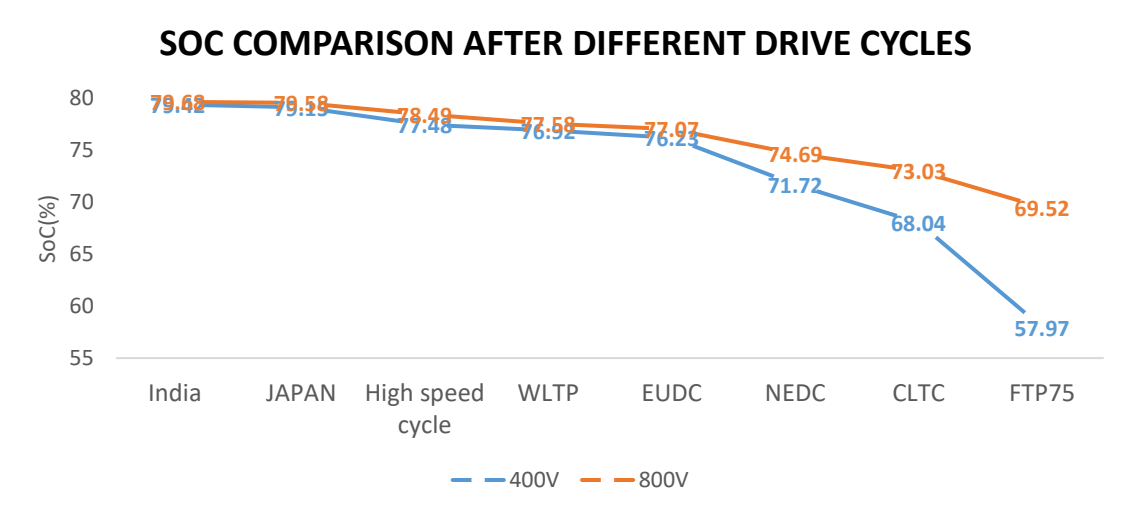

Figure 35. SoC comparison of 400V and 800V system after drive cycles.

According to the results, the 800V system has more SoC saving than 400V system. The most significant difference occurred in the FTP75 drive cycle, where the 800V system had 69.52% of the final SoC, compared to 57.97 for the 400V system, which was 11.55% more than the latter. In drive cycle FTP75, 800V system gains the more SoC saving of 11.55%, while on Indian drive cycle, there is very small difference of 0.26%.

Table 8 and **Figure 36** show the Max. DC current at different systems under different drive cycles. On China CLTC there is the biggest DC current on 400V system of 396.2A, with 100.4A on 800V system. Similar on FTP75 drive cycle, with 359A VS to 87.73 A. There is also a high DC current on High-speed drive cycle of 348.7 A on 400V system, compare to 126.4 A on 800V system.

Table 8. Max. DC current at different drive cycles.

Max. Current in the drive cycle (achieve the required speed)								
	India	JAPAN	High speed cycle	WLTP	EUDC	NEDC	CLTC	FTP75
400V (A)	63.3	129.1	348.7	78.48	156.3	155.9	396.2	359
800V (A)	17.31	36.81	126.4	19.03	62.69	63.43	100.4	87.73

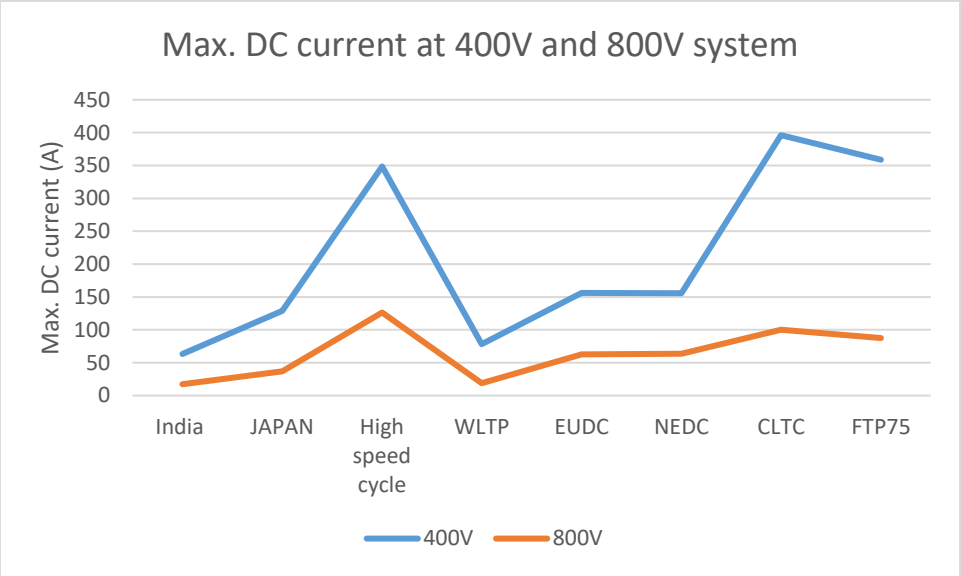

Figure 36. Max. DC current on 400V system VS 800V system.

As shown in Figure **37** the distance driven is also linearly related to the saving SoC in the 400V and 800V systems, such as the FTP75 drive cycle, which has the longest driving range, with the biggest SoC difference. But the shortest mileage is not the smallest gap, such as on Indian Dive cycle.

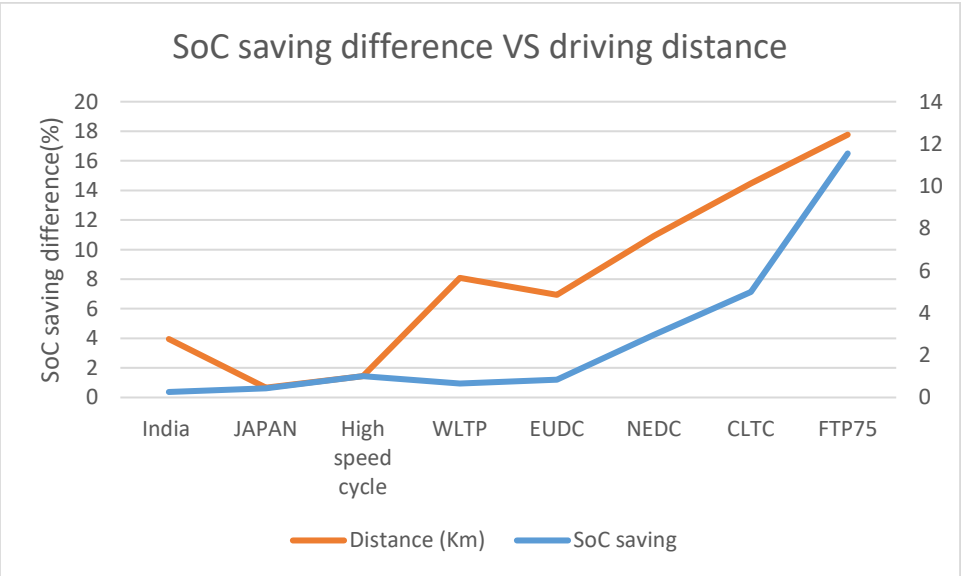

Figure 37. SoC saving difference VS Driving distance (Km).

Figure **38** shows the SoC difference vs. the maximum acceleration speed for each driving cycle, FTP75 driving cycle with the maximum acceleration speed has the largest SoC difference. The Indian drive cycle with minimal acceleration speed has the smallest SoC gap between 400V and 800V system. Since the current is especially lower in an 800V system during acceleration phase, the resistive losses in the wiring, motor, and other components are significantly reduced, while system energy efficiency increases. This efficiency leads to less energy being wasted as heat and therefore less drain on the battery, contributing to greater SoC savings. Similarity on regenerative braking mode, which 800v systems recover more energy back, because the reduced current (due to higher voltage) leads to fewer losses during the energy transfer from the motor to the battery, with less wasted as heat.

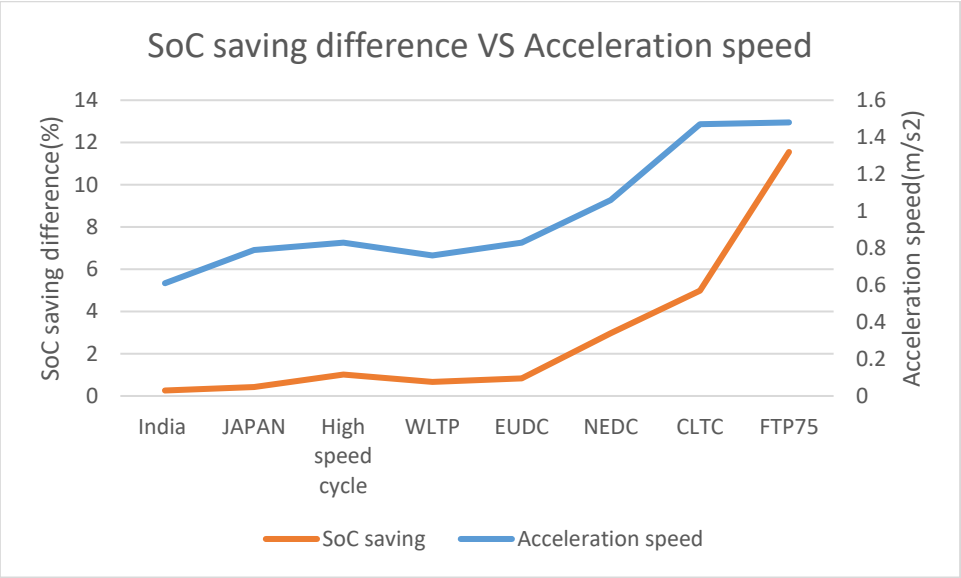

Figure 38. SoC saving difference VS acceleration speed.

Figure 39 shows the relationship between the SoC difference and the maximum speed of each driving cycle, and there is no obvious linear relationship between the driving cycle with the maximum speed and the SoC remaining. For example, the maximum speed of the high-speed drive cycle, and the EUDC drive cycle, their SoC remaining are not as large as the lower TOP speed WLTP and FTP75 drive cycles.

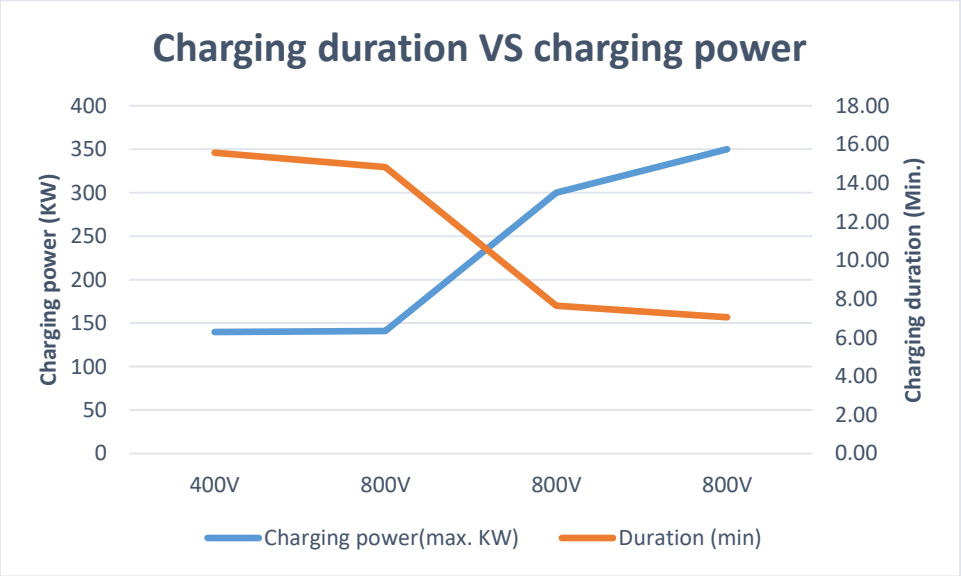

Figure 39. SoC saving difference VS Top Speed.

5.1 India Drive Cycle

This Indian drive cycle has a top speed of 42 km/h, which is like a typical slow driving scenario. The waveform of the results is shown in **Figure 40,** both systems reach the speed reference well, while 400V system has high torque and higher current results. Although the driving cycle time is relatively short, only 108s, the 800V system has acquired more energy saving, the final SoC result is about 0.26% less than the 400V system.

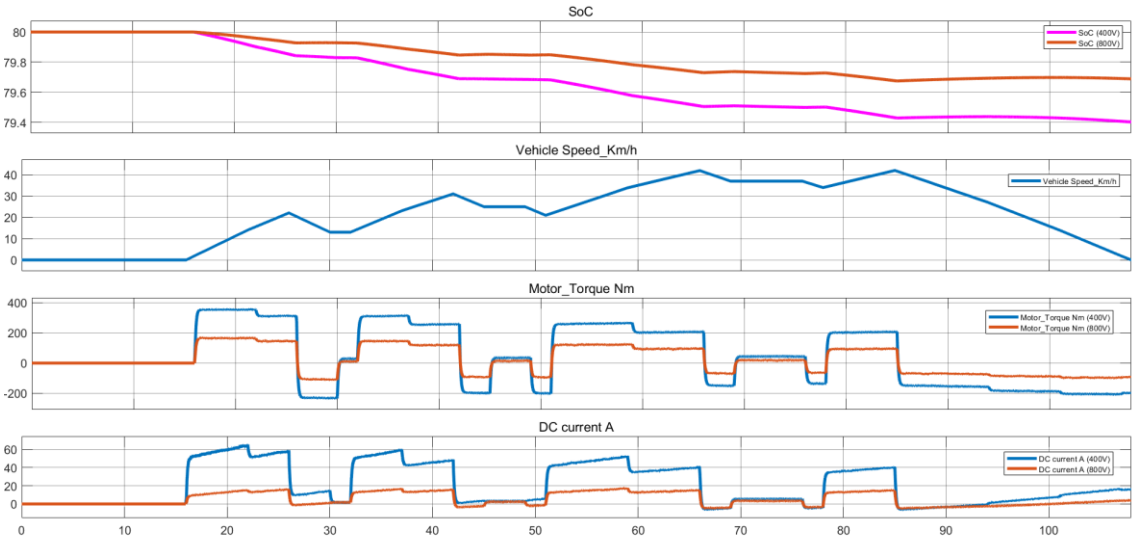

Figure 40. Waveform of 400V and 800V system in India Drive cycle.

5.2 Japanese 10 Mode Drive Cycle

The Japanese 10 mode drive cycle was used for emission certification of light duty vehicles in Japan. It simulates urban driving conditions. It covers 0.664 km at an average speed of 17.7 km/h and lasts 135 s. The maximum speed is 40 km/h.

The waveform of the results is shown in **Figure 41**, both systems reach the speed reference well, while 400V system has high torque and higher current results. After the drive cycle, the 400V system ends with SoC 79.15%, while 800V system ends with 79.58%.

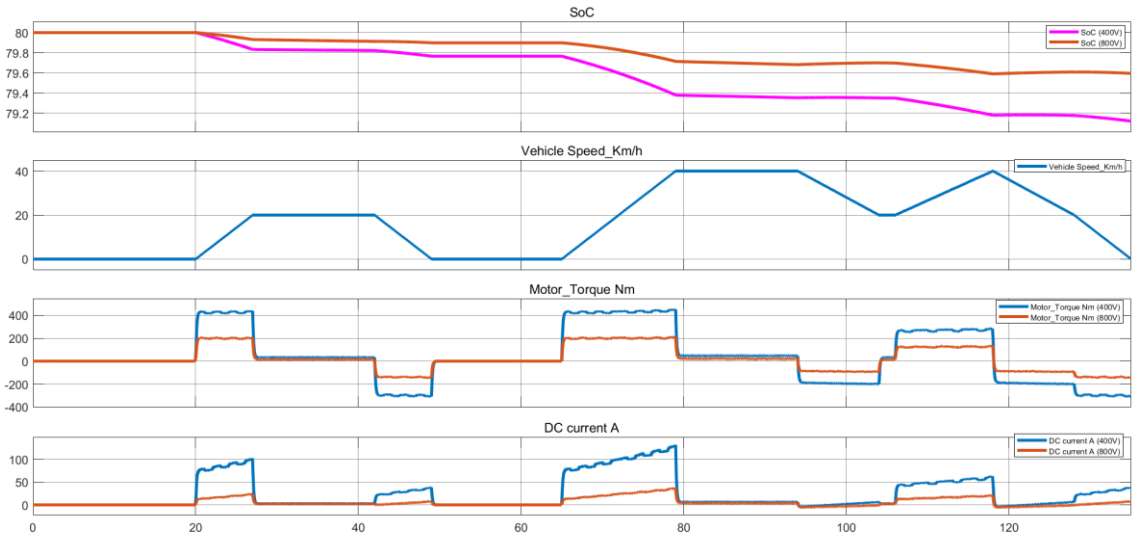

Figure 41. Waveform of 400V and 800V system in Japanese 10 mode drive cycle.

5.3 Specific High Speed Drive Cycle (120Km/h)

In this specific Drive cycle, the vehicle is accelerated to 120 km/h and then maintained at this steady high speed for a short time before decelerating to 0, duration of the drive cycle is 86 seconds. Results are shown in **Figures 42**.

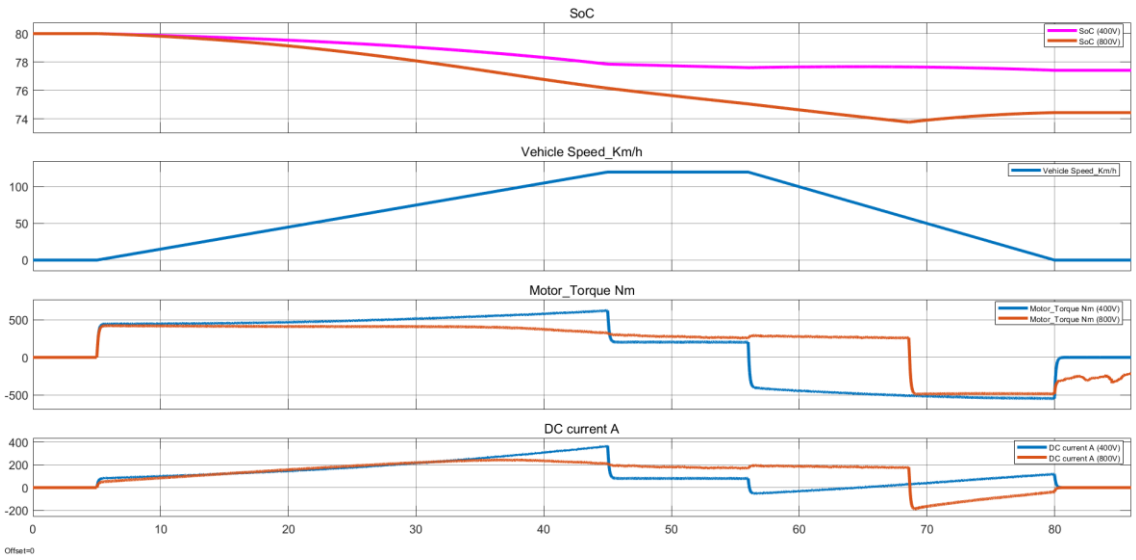

Figure 42. Waveform of 400V and 800V system in specific high speed drive cycle.

5.4 WLTP Class 1 Drive Cycle

WLTP, which stands for "World Light Vehicle Test Procedure", was jointly developed by Japan, United States, and the European Union, and its final version was officially codified in 2015. Compared to the old NEDC test, the test conditions for WLTC are significantly more complex. The average speed is 27.6 km/h, and the total test time was 1800s. Not only does it have a longer range, but the test time is also longer, and the acceleration and deceleration process during the test is more random. The results are shown in **Figure 43**, the 800V system reserves more energy savings of about 0.66% comparing to the 400V system.

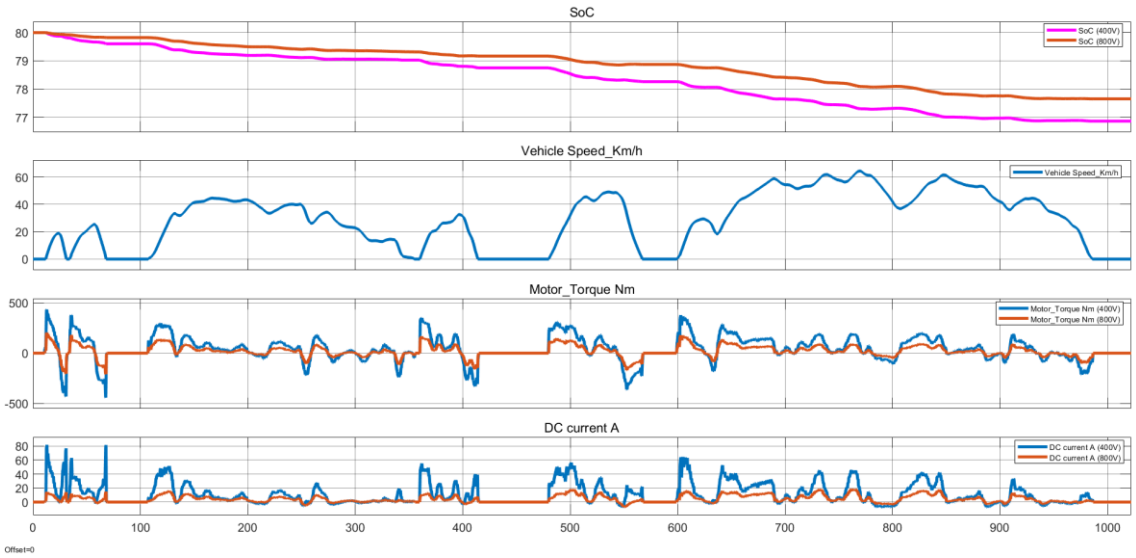

Figure 43. Waveform of 400V and 800V system in WLTP class 1 drive cycle.

5.5 EUDC Drive Cycle

The EUDC (Extra Urban Driving Cycle) segment was added after the fourth ECE (Economic Commission for Europe) cycle to account for more aggressive, high speed driving modes. The maximum speed of the EUDC cycle is 120 km/h, and the total duration is 400 s. **Figure 44** illustrates the test results of 400V system and 800V system. After 400s of

driving cycles, the SoC of the battery is maintained at 77.07% on 800V system. While the SoC ends with 76.23% on 400V system.

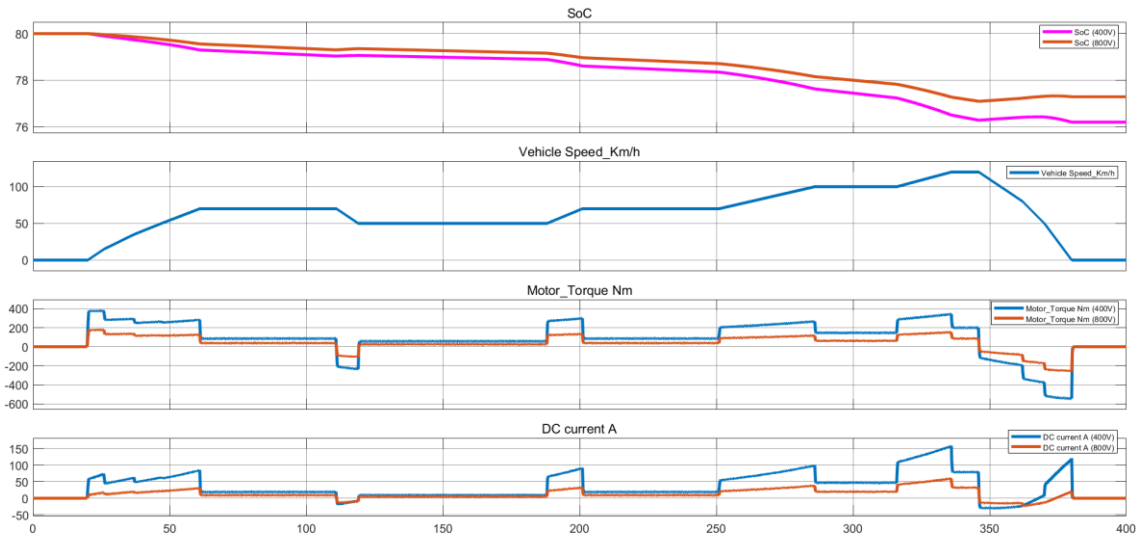

Figure 44. Waveform of 400V and 800V system in EUDC drive cycle.

5.6 NEDC Drive Cycle

The NEDC (New European Driving Cycle) is the European standard for endurance test conditions, which contains 4 urban cycles and 1 suburban cycle. NEDC working conditions are divided into two parts: urban working conditions and suburban working conditions. The urban operating conditions consisted of four ECE (Economic Commission for Europe) cycle units, with a maximum speed of 50 km/h and an average speed of 19 km/h during the test, each cycle time of 195 seconds, with a total distance of 4.052 km. The suburban test has a total of one EUDC cycle, with an average speed of 62.6km/h, an effective driving time of 400s, and a total distance of 6.955km. The NEDC condition is in a constant driving condition most of the time, and even in the process of acceleration and deceleration, the acceleration is constant, and the "speed-time" curve is very regular, which belongs to the category of steady-state conditions. **Figure 45** illustrates the test results of 400V system and 800V system after the 1180 s driving. 800V system gains 2.97% SoC savings than 400V system.

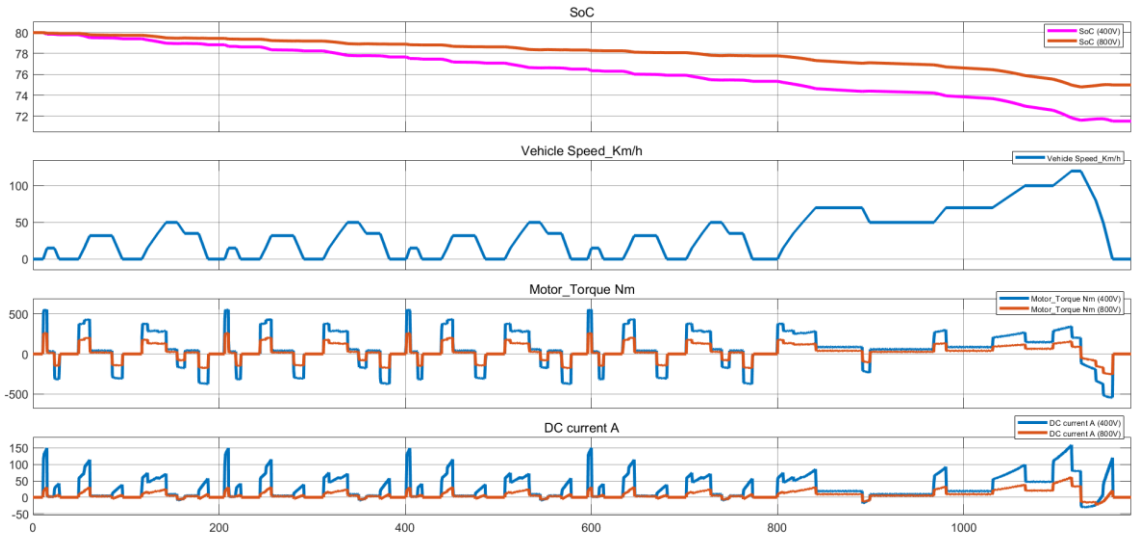

Figure 45. Waveform of 400V and 800V system in NEDC drive cycle.

5.7 China CLTC-P Drive Cycle

CLTC (China Light - Duty Vehicles Test Cycle) is a light vehicle driving condition standard for China's road traffic conditions and driving habits developed by China Automotive Research Center which was released in October 2019 and implemented in May 2020. The passenger car test condition CLTC-P (China light-duty vehicle test cycle-passenger car) includes three speed zones of low-speed, medium-speed and high-speed, with a total duration of 1800s, a total mileage of 14.480Km, a maximum speed of 114km/h, and an average speed of 28.96km/h. Compared with the WLTP cycle, the average speed of CLTC in urban, suburban and high-speed conditions is reduced to varying degrees, and the acceleration and deceleration process during the test is softer, but the peak deceleration is higher than that of WLTP, and the deceleration time is longer. **Figure 46** illustrates the test results of 400V system and 800V system. 800V system gains 4.99% SoC Saving than 400V system.

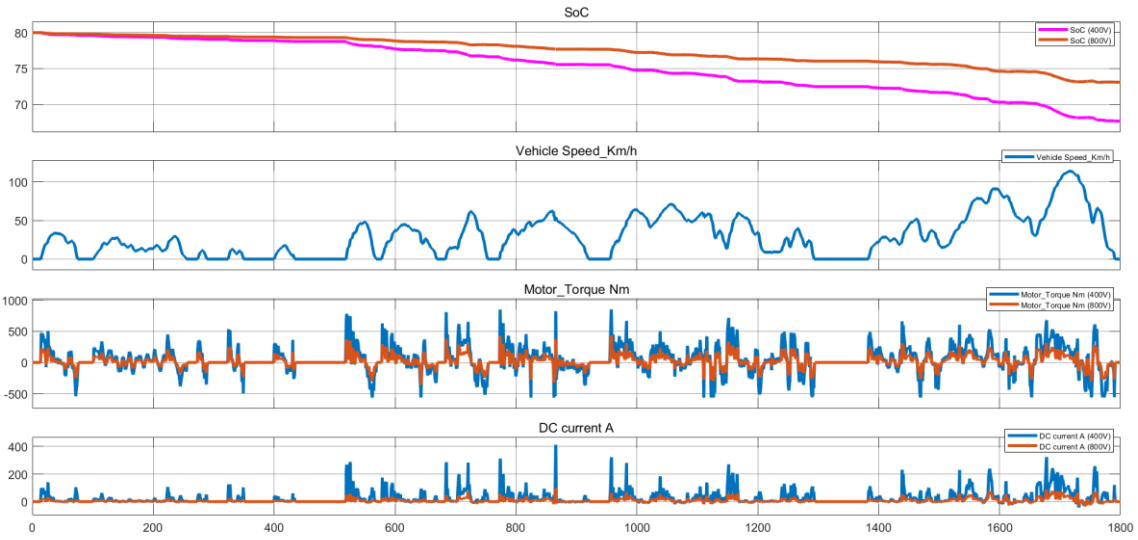

Figure 46. Waveform of 400V and 800V system in CLTC-P drive cycle.

5.8 FTP75 Drive Cycle

FTP75 (Federal Test Procedure) is a standard issued by the United States Energy Administration for testing the economy and emissions of passenger cars in urban conditions and is used to evaluate the emissions and fuel economy of light vehicles and light trucks. The full FTP75 cycle time is 1874s, the theoretical driving distance is 17.77 km, the average speed is 34.12 km/h, and the top speed is 91.25 km/h. **Figure 47** illustrates the test results of 400V system and 800V system. In this drive cycle, 800V gains 11.55% SoC savings than 400V system.

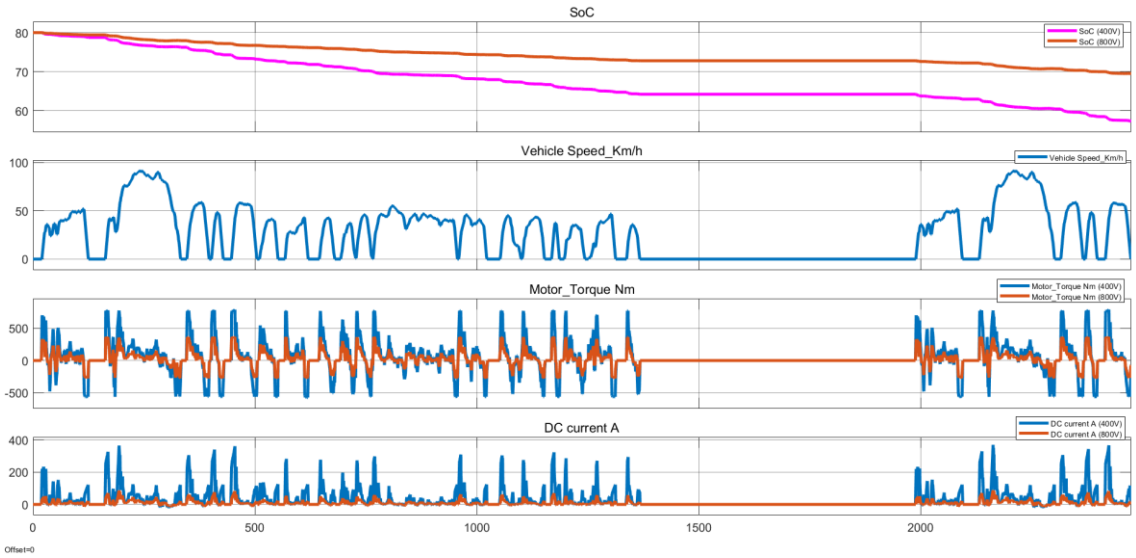

Figure 47. Waveform of 400V and 800V system in FTP75 drive cycle.

5.9 Battery Charging

In the simulation of charging efficiency, parameter of the charging power is set as in **Table 9**, the SoC changes of the battery were plotted, the system works well when starts with CC mode and switches to CV mode when battery voltage reaches pre-set charging voltage.

Table 9. Charging data summary of 400V and 800V charging voltage (40Kwh battery).

	400V	**800V**	**800V**	**800V**
Charging power(max.)	139.8KW	141KW	300KW	350KW
Charging voltage (max.)	466V	940V	1000V	1000V
Current (max.)	300A	150A	300A	350A
SoC initial	20%	20%	20%	20%
SoC end	90%	90%	90%	90%
Battery capacity	40Kwh	40Kwh	40Kwh	40Kwh
Duration (min.)	15.57	14.83	7.65	7.05

The results are shown in **Figure 48 to 52**. The 400V charging system charging the battery from 20% t0 90% within 15.57 minutes with charging power of 140KW, while the 800V

charging system charging the 800V System within 7.05 minutes with charging power rising to 350KW.

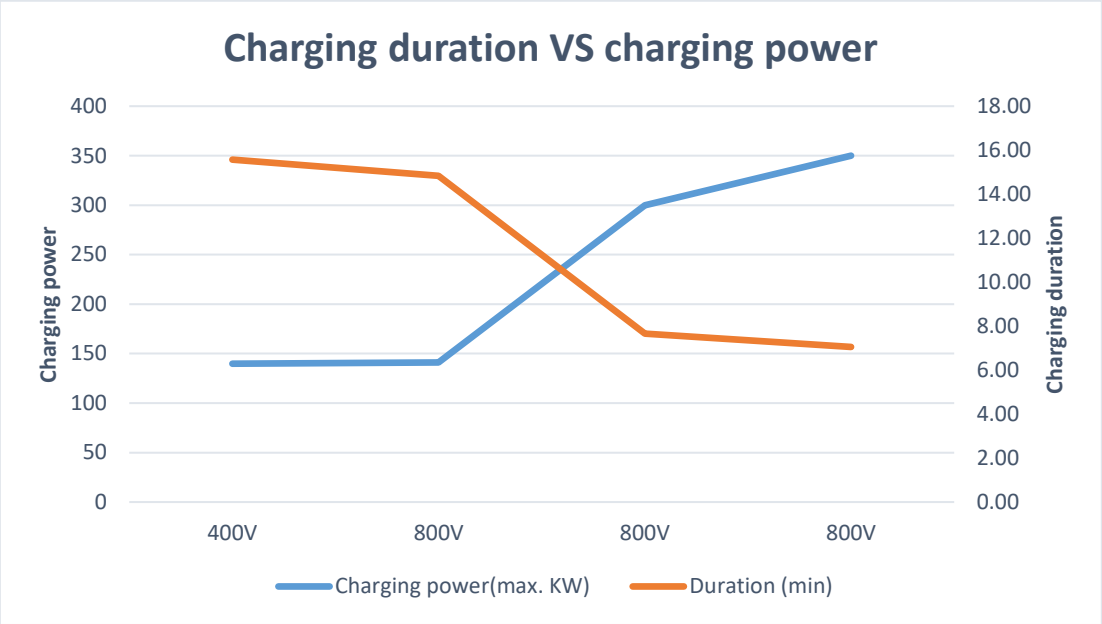

Figure 48. Battery charging duration VS charging power.

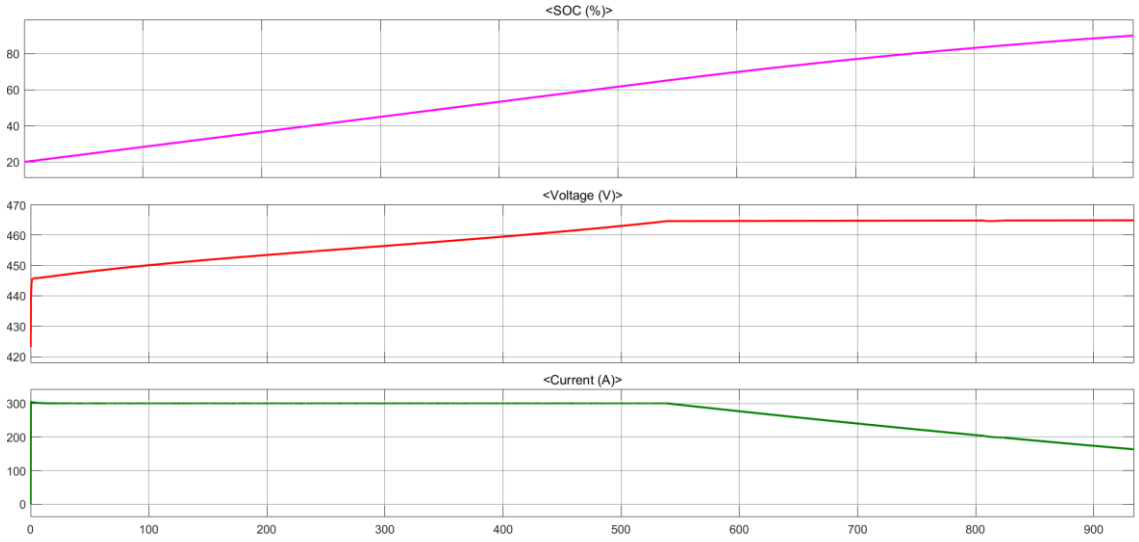

Figure 49. DC charging with 466V,300A for 400V battery.

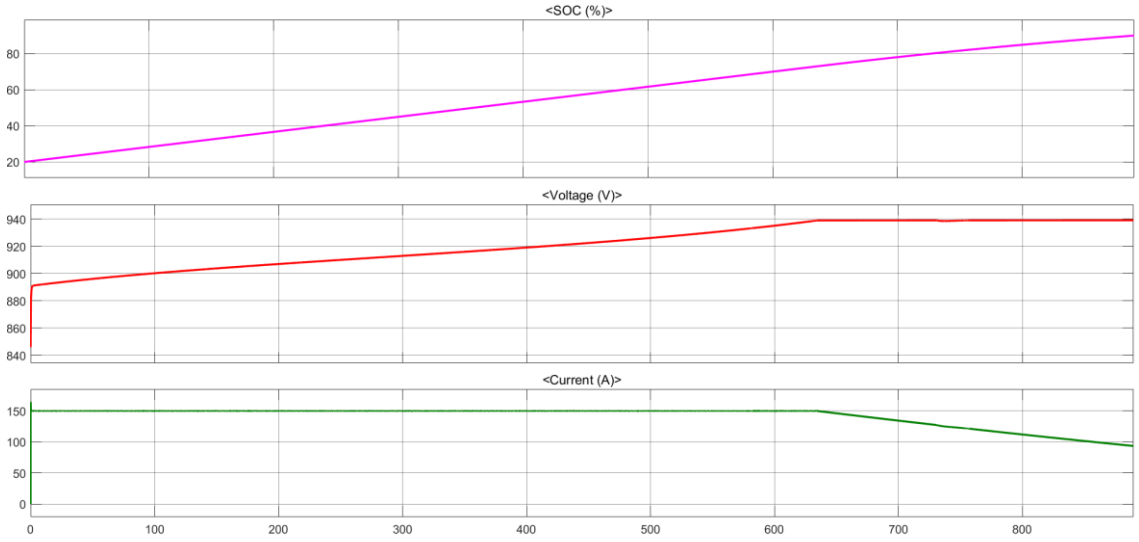

Figure 50. DC charging with 940V, 150A for 800V battery.

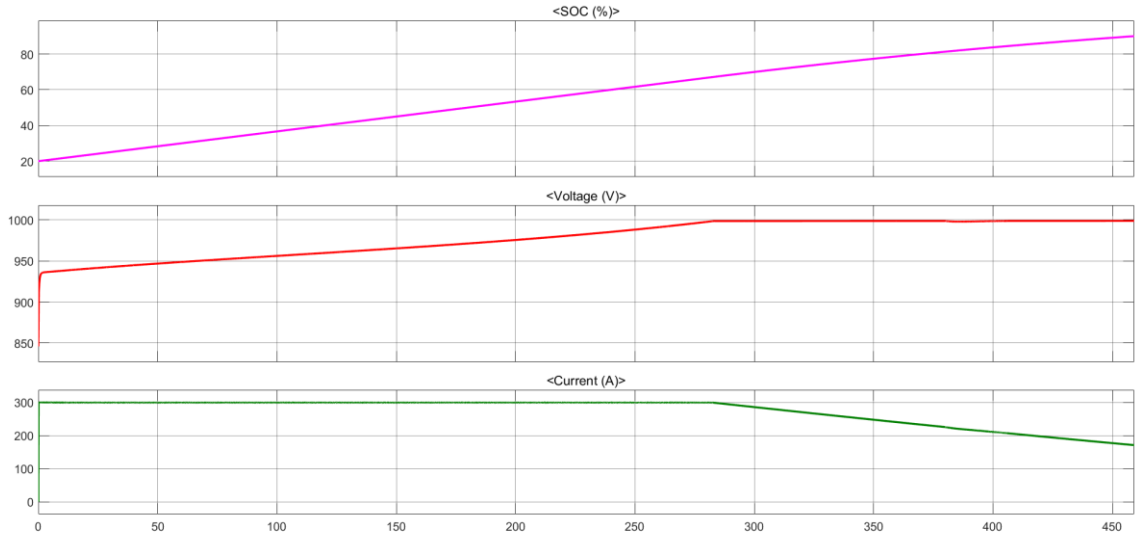

Figure 51. DC charging with 1000V, 300A for 800V battery.

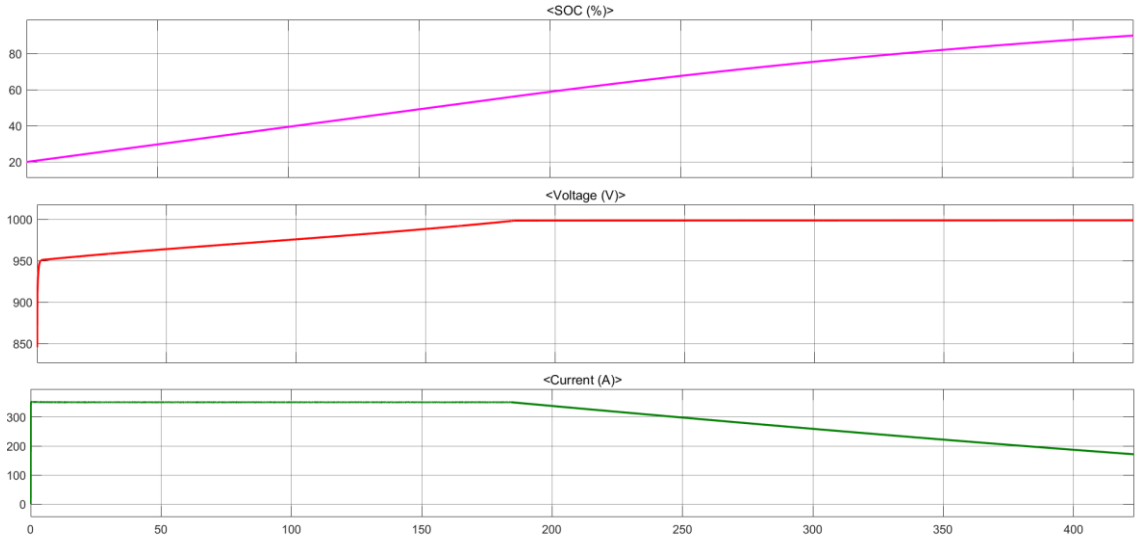

Figure 52. DC charging with 1000V, 350A for 800V battery.

6 Conclusion and Recommendation

Electrification is becoming the future trend of the automotive industry, which is not only conducive to reducing carbon emissions and impact of global climate change, but more importantly, it can improve energy efficiency, save energy, and improve the driving experience to attract more consumers to choose electric vehicles, and High voltage upgradation is becoming a key technology in this trend.

This paper reviews the characteristics of the main subsystems in electric vehicles, including batteries, electric motors, control systems, body and charging systems, and reviews different kinds of batteries and motors to select simulation schemes through literature review. The challenges to upgrade to 800V system have also been discussed, such as technological difficulties of battery, semiconductor, electronic components, and pressure on infrastructure.

By focusing on the simulations of BEV system and charging circuit under MATLAB Simulink, to understand the BEV and its battery charging philosophy. The performance of BEV system and charging system are verified under 400V and 800V levels, including the characteristics of energy consumption during different drive cycles, and battery charging speed under different charging power.

The results show that the 800V system recorded more SoC savings overall than the 400V system over the 8 driving cycles. The largest SoC savings occurred on the FTP75 driving cycle, where the 800V system saved up to 11.55% compared to the 400V SoC after a 17.77km cycle of 1874 seconds, also with significant differences of 14.48% and 10.93% on the CLTC and NDEC driving cycles, respectively. Comparing the characteristics of each driving cycle, the most relevant is the effect of acceleration speed, the FTP75 driving cycle with maximum acceleration speed (1.48m/s^2) saves more energy in the 800V system, and there is also a certain correlation in the driving distance, while the high speed of the cycle is not significantly influencing the results. This is also reflected in the

DC current in the system, which can be much smaller on 800V system than that in a 400V system to achieve the maximum speed in the cycle, without affecting the power output.

For the charging speed, the charging power of 141KW, 300KW and 350KW of 800V system is increased by more than 2 times than 139.8KW of 400V system under the typical CC-CV charging mode. If to keep maximum charging current the same, the high-voltage system can be charged with even more power in less time, which conclude that the charging power can be increased by increasing the charging voltage while the cable specifications remain the same.

Although the basic goal has been achieved, the controlling models could be further optimized to improve realization. And, due to the problem of workload and time, there are many details that can be further optimized and improved for the control strategy of the system and specific simulations, such as the high-speed motor application, more advance PMSM controlling strategy, lookup table method, high-frequency inverter application and battery temperature influence. Furthermore, the solution to challenges can be more deeply reviewed with the latest development progress. Finally, due to professional and tools limitations, many other parameters of electric vehicles are not considered in this paper, and there are other topics could be planned for further studies, such as the performance and energy loss on new silicon carbide (SiC) switching components, comparing the IGBT devices, reducing the impact to the grid by the high voltage charging stations with integrating of battery energy storage system, and the vehicle electric system isolation technology analysis for endure safety working under the high voltages.

7 References

Abulifa, A., Ahmad, R. R., Soh, A. C., Radzi, M., & Hassan, M. (2017). Modelling and Simulation of Battery Electric Vehicle by Using MATLAB-Simulink. *2017 IEEE 15th Student Conference on Research and Development (SCOReD)*, (pp. 383-387).

Aghabali, I., Bauman, J., Kollmeyer, P., Wang, Y., Bilgin, B., & Emadi, A. (2020). 800V Electric Vehicle Powertrains: Review and Analysis of Benefits, Challenges, and Future Trends. . *IEEE Transactions on Transportation Electrification*, (p. 1).

Aghabali, I., Kollmeyer, P. J., & Bilgin, B. (2021). 800-V Electric Vehicle Powertrains: Review and Analysis of Benefits, Challenges and Future Trends. *IEEE TRANSACTIONS ON TRANSPORTATION ELECTRIFICATION*, VOL. 7,.

Aiso, K., & Akatsu, K. (2022). Performance Comparison of High-Speed Motors for Electric Vehicle. *world electric vehicle journal*, 13.

Allca-Pekarovic, A., Kollmeyer, P. J., Mahvelatishamsabadi, P., Mirfakhrai, T., Naghshtabrizi, P., & Emadi, A. (2024). Loss Modeling and Testing of 800-V DC Bus IGBT and SiC Traction Inverter Modules. *IEEE Transactions on Transportation Electrification*, 2923-2935.

Alves, L. F., Gomes, R. C., Lefranc, P., Pegado, R. D., & Jeannin, P.-O. (2017). SIC power devices in power electronics: An overview. *Brazilian Power Electronics Conference (COBEP)*, (pp. 1-8). Juiz de Fora.

Arancibia, A., & Strunz, K. (2012). Modeling of an Electric Vehicle Charging Station for Fast DC Charging. *International Electric Vehicle Conference,*, (pp. 1-6). SC.

Audi. (2018). *High voltage battery.*

BAI, A. S., & Sealy, M. (2023). *Ten Reasons an Electric Motor is better than an Internal Combustion Engine [ICE] for our car transportation*. Retrieved from The Irish Electric Vehicle Association: https://www.irishevassociation.ie/news/ten-reasons-an-electric-motor-is-better-than-an-internal-combustion-engine-ice-for-our-car-transportation

Banuri, S. H., Qayyum, U., Qureshi, K. R., & Ahmed, A. (2020). Investigation of Drag Coefficients for Various Car Models. *17th International Bhurban Conference on Applied Sciences and Technology (IBCAST),*, (pp. 467-471). Islamabad, Pakistan.

Barzegarkhoo, R., Farhangi, M., Lee, S. S., Siwakoti, Y. P., & Frede Blaabjerg. (2024). Chapter 5 - Switched-boost-based multilevel inverters. In F. Blaabjerg, *Control of Power Electronic Converters and Systems,* (pp. 127-154). Academic Press.

Bates, A. M., Preger, Y., Torres-Castro, L., Harrison, K. L., Harris, S. J., & John Hewson. (2022). Are solid-state batteries safer than lithium-ion batteries? *Joule*, 742-755.

Bellur, D. M., & Kazimierczuk, M. K. (2007). DC-DC converters for electric vehicle applications. *2007 Electrical Insulation Conference and Electrical Manufacturing Expo*, (pp. 286-293). Nashville.

Blink. (2022). *What Are the Different Methods of Charging an Electric Vehicle?* Retrieved from Blinkcharging: https://blinkcharging.com/blog/what-are-the-different-methods-of-charging-an-electric-vehicle

Bonnen Battery. (2023, July 6). *High-Voltage Cables for Electric Vehicles (EVs) – Everything You Need to Know*. Retrieved from Bonnen Battery: https://www.bonnenbatteries.com/high-voltage-cables-for-electric-vehicles-evs-everything-you-need-to-know/

Cao, Z., Mahmoudi, A., Kahourzade, S., & W. L. Soong. (2021). An Overview of Electric Motors for Electric Vehicles. *021 31st Australasian Universities Power Engineering Conference (AUPEC),* , (pp. 1-6,). Perth.

Carter, S. R., I, P. P., Varadhan, N. V., Kowshik, S., Gopinath, G., & G, J. S. (2023). Field-Oriented Control (FOC) for Permanent Magnet Synchronous Motors (PMSM) In Electric Vehicle. *2023 IEEE International Conference on Next Generation Electronics (NEleX 2023).*

Cheng, M., Sun, L., Buja, G., & Song, L. (2015). Advanced Electrical Machines and Machine-Based Systems for Electric and Hybrid Vehicles. *Energies*, 9541-9564.

China, R. i. (2022). *800V High Voltage Platform Research Report.*

Conlon, B., Anwar, M., Sevel, K., Wang, M., Badawi, R., & A. Bavili. (2022). Switchable 400V/800V High Voltage Architecture for Ultium Battery Electric Trucks. *IEEE Energy Conversion Congress and Exposition (ECCE)*, (pp. 1-6). Detroit, MI, USA.

Copper Development Association INC. (2022, July 21). *Copper in electric vehicles*. Retrieved from Copper Development Association INC: https://www.copper.org/environment/sustainable-energy/electric-vehicles

D, Y. S., R, S. H., & G, N. H. (2023). Electric Vehicle with Regenerative Braking Model using MATLAB - Simulink. *2023 IEEE Renewable Energy and Sustainable E-Mobility Conference (RESEM) .*

Electric vehicle database. (2023). *Range of full electric vehicles*. Retrieved from Electric vehicle database: https://ev-database.org/cheatsheet/range-electric-car

Electrify News. (2023, August). *How Long It Takes To Charge An Electric Car at a Charging Station*. Retrieved from Electrify News: https://electrifynews.com/news/ev-chargers/how-long-does-it-take-to-charge-an-electric-car-at-a-charging-station/

Engineering. (2023, 8 14). *High Voltage Vehicles: Why 800-Volt EVs are on the Rise*. Retrieved from Engineering.com: https://www.engineering.com/high-voltage-vehicles-why-800-volt-evs-are-on-the-rise

EVbox. (2023, 5 4). *Electric car battery weight explained*. Retrieved from EVbox: https://blog.evbox.com/ev-battery-weight

EVbox. (2023, April 14). *EV charging: the difference between AC and DC*. Retrieved from EVBox Blog: https://blog.evbox.com/difference-between-ac-and-dc

EVEsco. (2023). *The ultimate guide to DC fast charging*. Retrieved from EVEsco: https://www.power-sonic.com/blog/the-ultimate-guide-to-dc-fast-charging/

Furcher, T., Giraldo, I. H., Rupalla, F., & Smith, A.-S. (2023, 7 28). *Electric-vehicle buyers demand new experiences*. Retrieved from McKinsey & Company: https://www.mckinsey.com/industries/automotive-and-assembly/our-insights/electric-vehicle-buyers-demand-new-experiences

Hailin, Z., Shirong, Y., hongtao, L., Zhan, L., & Fuyuan, Z. (2019). Research on brake energy recovery of permanent magnet synchronous motor in electric vehicle . *Journal of Fuzhou University (Natrual Science Edition)*, Vol.47, No.4.

HASAN, F., & ISLAM, M. R. (2022). New Energy Vehicles from the Perspective of the Market and Environment. *Business Strategy Finance and Managemen*, 38-51.

IEA. (2024). *Trends in electric cars*. Retrieved from IEA: https://www.iea.org/reports/global-ev-outlook-2024/trends-in-electric-cars

Jung, C. (2017). Power Up with 800-V Systems: The benefits of upgrading voltage power for battery-electric passenger vehicles. *IEEE Electrification Magazine*, 53-58.

Kane, M. (2023, November). *ChargePoint Introduces New 500 kW Ultra-Fast DC Charging System*. Retrieved from Inside EVs: https://insideevs.com/news/696420/chargepoint-500kw-dc-fast-charging-system/

Khan, M. S., Nag, S. S., Das, A., & Yoon, C. (2021). A Novel Buck-Boost Type DC-DC Converter Topology for Electric Vehicle Applications. *IEEE Energy Conversion Congress and Exposition*, (pp. 1534-1539). Vancouver.

Kohei, A., & Kan, A. (2020). High Speed SRM Using Vector Control for Electric Vehicle. *CES TRANSACTIONS ON ELECTRICAL MACHINES AND SYSTEMS*, 61-67.

Krings, A., & Monissen, C. (2020). Review and Trends in Electric Traction Motors for Battery Electric and Hybrid Vehicles. *24th International Conference on Electrical Machines (ICEM).* Gothenburg.

Kucevic, D., Truong, C. N., Jossen, A., & Hesse, H. C. (2018). Lithium-Ion Battery Storage Design for Buffering Fast Charging Stations for Battery Electric Vehicles and Electric Buses. *Conference on Sustainable Energy Supply and Energy Storage Systems*, (pp. 1-6). Hamburg, Germany.

Lamm, D.-I. A. (2019). *Future eDrive-Technologies with Focus on Battery Design Options.* e-Technologies GmbH.

Li, J., Tang, C., Wang, Y., Zhou, X., & Linwei Sai. (2024). Possibility of defective monolayer graphene as potential anode material of metal-ion batteries. *Materials Today Communications*, Volume 40.

Liao, F., Molin, E., & van Wee, B. (2016). Consumer preferences for electric vehicles: a literature review. *Transport Reviews,*, 37(3), 252–275.

Liu, H., Liu, C., Zhou, Y., Zhang, Y., Deng, W., Zou, G., . . . Ji, X. (2024). The application of Al2O3 in separators and solid electrolytes of lithium-ion battery: A review. *Energy Storage Materials*, volume 71.

López, I., Ibarra, E., Matallana, A., Andreu, J., & Kortabarria, I. (2019). Next generation electric drives for HEV/EV propulsion systems: Technology, trends and challenges. *Renewable and Sustainable Energy Reviews*.

Lulhe, A. M., & Date, P. T. (2015). A Design & MATLAB Simulation ofMotor Drive used for Electric Vehicle. *2015 International Conference on Control,Instrumentation, Communication and Computational Technologies (ICCICCT).*

Lüthje, J., Zhang, Z., Carmen, M., & Andersen, M. (2018). Analysis and Design of a dc-dc Converter Using Visual Aid. *IEEE International Power Electronics and Application Conference and Exposition (PEAC)*, (pp. 1-6).

Marklines. (2024). *Electric Vehicle (BEV/PHV/FCV) Sales Monthly Report.* Marklines.

MarkLines. (n.d.). *Comparison Data of 12 Traction Motors of Major Electric Vehicles*. Retrieved from https://www.marklines.com/en/teardown/drive_motor

Monika. (2023). *Skyworth Auto introduces 800V+4C supercharging tech, AI-enabled Q&A system*. Retrieved from Gasgoo.com: https://autonews.gasgoo.com/new_energy/70024693.html

Nayak, S., Bohre, A. K., & Kumar, P. (2022). Modeling and Performance Analysis of an Electric Vehicle. *2022 International Conference on Smart Generation Computing, Communication and Networking.* Karnataka, India.

Panasonic Industry. (2023). *What is an inverter on an electric vehicle?* Retrieved from Panasonic Industry: https://industrial.panasonic.cn/ea/ss/technical/ap6

Pesaran, A. A. (2023). Lithium-Ion Battery Technologies for Electric Vehicles: Progress and challenges. *IEEE Electrification Magazine*, 35-43.

Prasad, R., Namuduri, C., & Gopalakrishnan, S. (2023). On-Demand Battery Reconfiguration for 800V DC Fast Charging in Electric Vehicles. *IEEE Energy Conversion Congress and Exposition (ECCE)*, (pp. 5140-5145). Nashville, TN, USA.

Rahul Rao. (2021, May 26). *Chart: Behind the Three-Decade Collapse of Lithium-Ion Battery Costs*. Retrieved from IEEE spectrum: https://spectrum.ieee.org/chart-behind-the-three-decade-collapse-of-lithium-ion-battery-costs

Sambhavi, Y. V., & Vijayapriya Ramachandran. (2023). A technical review of modern traction inverter systems used in electric vehicle application. *Energy Reports*, 3882-3907.

Sburlan, I. C., Vasile, I., & Tudor, E. (2021). Comparative study between semiconductor power devices based on silicon Si, silicon carbide SiC and gallium nitrate GaN used in the electrical system subassembly of an electric vehicle. *International Semiconductor Conference (CAS)*, (pp. 107-110). Romania,.

Schneider, D. (2019). Silicon anodes will give lithiumion batteries a boost. *IEEE Spectrum*, 48-49.

Shen, W., Vo, T. T., & Kapoor, A. (2012). Charging Algorithms of Lithium-Ion Batteries: an Overview. *7th IEEE Conference on Industrial Electronics and Applications (ICIEA)*, (pp. 1567-1572).

Shi, B., Ramones, A. I., Liu, Y., Wang, H., Li, Y., Pischinger, S., & Andert, J. (2023). A review of silicon carbide MOSFETs in electrified vehicles: Application, challenges, and future development. *IET Power Electronics*, 2103-2120.

Singh, A. K., Chaudhari, M. A., Sekhar, K. S., & Kumar, R. (2023). Analysis of Isolated DC-DC Converters for Electric-Vehicle (EV) Battery Charging. *IEEE Renewable Energy and Sustainable E-Mobility Conference (RESEM)*, (pp. 1-6). Bhopal, India.

Tarascon, J.-M., & Armand, M. (2001). Issues and challenges facing rechargeable lithium batteries. *Nature* , 359–367.

Tesla Model 3 (facelift 2023) 60 kWh (283 Hp) . (2024). Retrieved from Wiki Automotive Catalog: https://www.auto-data.net/en/tesla-model-3-facelift-2023-60-kwh-283hp-49902

TOSHIBA. (2020). *Comparison of SiC MOSFET and Si IGBT.* Toshiba Electronic Devices & Storage Corporation.

Tredeau, F. P., & Salameh, Z. M. (2009). Evaluation of Lithium iron phosphate batteries for electric vehicles application. *IEEE Vehicle Power and Propulsion Conference*, (pp. 1266-1270). Dearborn.

Wang, Y. (2022). Research on the Performance Test of Lithium Ion Battery Anode Based on Energy Density Optimization Technology of Layered Cathode Material. *6th*

International Conference on Power and Energy Engineering (ICPEE), (pp. 344-350). Shanghai, China.

Wikipedia. (2024). *History of the electric vehicle*. Retrieved from Wikipedia: https://en.wikipedia.org/wiki/History_of_the_electric_vehicle

Worldwide Harmonized Light Vehicles Test Cycle (WLTC). (2019). Retrieved from Emission test cycles: https://dieselnet.com/standards/cycles/wltp.php

Wu, Q., Zhang, B., & Lu, Y. (2022). Progress and perspective of high-voltage lithium cobalt oxide in lithium-ion batteries. *Journal of Energy Chemistry*, 283-308.

www.evehicletechnology.com. (2021). Retrieved from www.evehicletechnology.com

X-engineering. (2015). *What is a DC-DC converter ?* Retrieved from X-engineering: https://x-engineer.org/dc-dc-converter/

Yepeng Wang. (2022). Research on the Performance Test of Lithium Ion Battery Anode Based on Energy Density Optimization Technology of Layered Cathode Material. *6th International Conference on Power and Energy Engineering (ICPEE)*, (pp. 344-350). Shanghai.

Ying, T.-K., Gao, X.-P., Hu, W.-K., Wu, F., & Noréus, D. (2006). Studies on rechargeable NiMH batteries. *International Journal of Hydrogen Energy*, 525-530.

(n.d.). *Yole market research.*

Yu, X., Chen, R., Gan, L., Li, H., & Liquan Chen. (2023). Battery Safety: From Lithium-Ion to Solid-State Batteries. *Engineering*, 9-14.

Yuexian, L., Tianyu, W., Yayu, Y., & Xiaoru, W. (2014). Modeling and simulation of electric vehicles' charge and discharge system . *Power System Protection and Control*, Vol.42 No.13.

Zhang, P., Du, Y., Habetler, T. G., & Lu, B. (2009). A survey of condition monitoring and protection methods for medium voltage induction motors. *IEEE Energy Conversion Congress and Exposition*, (pp. 3165-3174). San Jose, CA, USA.

8 Appendices

8.1 Appendix 1. Specific High speed drive cycle data(120Km/h)

TIME(s)	SPEED(Km/h)
1	0
2	0
3	0
4	0
5	0
6	3
7	6
8	9
9	12
10	15
11	18
12	21
13	24
14	27
15	30
16	33
17	36
18	39
19	42
20	45
21	48
22	51
23	54
24	57
25	60
26	63
27	66
28	69
29	72
30	75
31	78
32	81
33	84
34	87
35	90
36	93
37	96

38	99
39	102
40	105
41	108
42	111
43	114
44	117
45	120
46	120
47	120
48	120
49	120
50	120
51	120
52	120
53	120
54	120
55	120
56	120
57	115
58	110
59	105
60	100
61	95
62	90
63	85
64	80
65	75
66	70
67	65
68	60
69	55
70	50
71	45
72	40
73	35
74	30
75	25
76	20
77	15
78	10
79	5
80	0
81	0
82	0

83	0
84	0
85	0
86	0